

REPORT DOCUMENTATION F


AD-A254 267

0188

Public reporting burden for this collection of information is estimated to average 1 hour per gathering and maintaining the data needed, and completing and reviewing the collection of collection of information, including suggestions for reducing this burden, to Washington in Davis Highway, Suite 1204, Arlington, VA 22202-4302, and to the Office of Management and



1. In data sources, the aspect of this is, 1215 Jefferson 1503

1. AGENCY USE ONLY (Leave blank)		2. REPORT DATE Summer 92	3. REPORT TYPE AND DATES COVERED THESIS/DISSERTATION	
4. TITLE AND SUBTITLE A Comparison of Radar Rainfall Estimates and Rain Gage Measurements During Two Denver Thunderstorms			5. FUNDING NUMBERS	
6. AUTHOR(S) David Joseph Speltz, Captain				
7. PERFORMING ORGANIZATION NAME(S) AND ADDRESS(ES) AFIT Student Attending: Colorado State University			8. PERFORMING ORGANIZATION REPORT NUMBER AFIT/CI/CIA- 92-070	
9. SPONSORING/MONITORING AGENCY NAME(S) AND ADDRESS(ES) AFIT/CI Wright-Patterson AFB OH 45433-6583			10. SPONSORING/MONITORING AGENCY REPORT NUMBER	
11. SUPPLEMENTARY NOTES				
12a. DISTRIBUTION/AVAILABILITY STATEMENT Approved for Public Release IAW 190-1 Distributed Unlimited ERNEST A. HAYGOOD, Captain, USAF Executive Officer			12b. DISTRIBUTION CODE	
13. ABSTRACT (Maximum 200 words)				
<p><b>DTIC</b> <b>SELECTE</b> <b>AUG 25 1992</b></p> <p><b>S B D</b></p> <p><b>92-23503</b></p> <p><b>92 8 24 012</b></p> 				
14. SUBJECT TERMS			15. NUMBER OF PAGES 83	
			16. PRICE CODE	
17. SECURITY CLASSIFICATION OF REPORT	18. SECURITY CLASSIFICATION OF THIS PAGE	19. SECURITY CLASSIFICATION OF ABSTRACT	20. LIMITATION OF ABSTRACT	

THESIS

A COMPARISON OF RADAR RAINFALL ESTIMATES AND RAIN GAGE  
MEASUREMENTS DURING TWO DENVER THUNDERSTORMS

Submitted by

David Joseph Speltz

Atmospheric Science Department

In partial fulfillment of the requirements

for the Master of Science

Colorado State University

Fort Collins, Colorado

Summer 1992

COLORADO STATE UNIVERSITY

May 7, 1992

WE HEREBY RECOMMEND THAT THE THESIS PREPARED UNDER OUR SUPERVISION BY DAVID JOSEPH SPELTZ ENTITLED A COMPARISON OF RADAR RAINFALL ESTIMATES AND RAIN GAGE MEASUREMENTS DURING TWO DENVER THUNDERSTORMS BE ACCEPTED AS FULFILLING IN PART REQUIREMENTS FOR THE DEGREE OF MASTER OF SCIENCE.

Committee on Graduate Work

\_\_\_\_\_  
*Freeman M. Smith*

\_\_\_\_\_  
Stan A. Ruffel

\_\_\_\_\_  
*J. M. K.*

Adviser

\_\_\_\_\_  
*Stephen R. Cox*

Department Head

DTIC QUALITY INSPECTED 2

Accession For	
NTIS GRA&I	<input checked="" type="checkbox"/>
DTIC TAB	<input type="checkbox"/>
Unannounced	<input type="checkbox"/>
Justification	
By _____	
Distribution/	
Availability Codes	
Dist	Avail and/or Special
A-1	

## ABSTRACT

### A COMPARISON OF RADAR RAINFALL ESTIMATES AND RAIN GAGE MEASUREMENTS DURING TWO DENVER THUNDERSTORMS

It has long been hoped that rainfall measurements made with weather radars would be able to supplement or even replace rain gage networks. During the summer of 1991 Colorado State University's (CSU) Department of Atmospheric Science participated in an experiment which was intended, in part, to determine how useful radar measurements are in helping to estimate heavy rainfall from thunderstorms. A dense array of 41 automatic rain gages operated by the Denver Urban Drainage and Flood Control District (UDFCD) provided precipitation measurements to compare with the radar results. Two thunderstorms were observed: the first occurred on June 6 and produced up to 43.7 mm (1.72 in) of rain in 85 minutes, while the August 5 storm resulted in peak rainfall amounts of 37.8 mm (1.49 in) in 60 minutes.

Unfortunately, estimates of rainfall made by using a relation between the radar measured reflectivity (Z) and the rain rate (R) are frequently in error by large amounts. The radar estimate over gage 540 during the June 6 storm was 58.8 mm (2.31 in) higher than the gage amount, an error of 201%. During the August 5 event gage 1720 recorded 37.8 mm, while the radar estimate was 27.8 mm (1.09 in) lower. Such large errors are unacceptable for most meteorological or hydrological purposes. The use of different Z-R relations provided overall improvement during both storms, while reflectivity thresholds resulted in better estimates during the June 6 storm, in which hail was present.

During the June 6 storm the worst of the overestimates were associated with unusually high reflectivity values resulting from the presence of hail. Hail was inferred from an examination of reflectivity ( $Z$ ), differential reflectivity ( $Z_{DR}$ ), hail detection signal ( $H_{DR}$ ), and difference reflectivity ( $Z_{DP}$ ) fields. Values of  $Z > 50$  dBZ, near-zero  $Z_{DR}$  measurements, positive  $H_{DR}$  values, and  $Z_{DP}$  values deviating from the rain line all provide evidence for the presence of hail. Using a reflectivity threshold of 50 dBZ, in an attempt to account for hail contamination, improves the average ratio of total gage rainfall to radar estimated rainfall ( $G/RA$ ) from 0.77 to 0.92. The average difference improved from 8.0 mm to 3.5 mm, while the percentage difference dropped from 87.5% to 54.4%.

Even though overall results improve with the use of a threshold during the June 6 event, the danger of badly underestimating rainfall in a storm with  $>50$  dBZ values and no hail is very real. This is shown to be the case during the August 5 event: rainfall estimates were too low without a threshold, a 50 dBZ cap only increased the errors. Measurements of  $Z_{DR}$ ,  $H_{DR}$ , and  $Z_{DP}$  all indicated the absence of hail during this storm. Even radars able to make the polarimetric measurements used here cannot account for the effects of evaporation and wind drift below the beam level. This study confirms what many previous studies have shown: radar rainfall estimates using the Z-R relations tested here provide good supplemental information, but will not completely replace traditional rain gages.

David Joseph Speltz  
Atmospheric Science Department  
Colorado State University  
Fort Collins, CO 80523  
Spring 1992

## DEDICATION

I would like to dedicate this thesis to my wife Tami. The extra hours I spent working during the evenings and frequently on weekends were often harder on Tami than on me. She managed to endure the hours we spent apart with grace and understanding, which helped make my job a lot easier. Tami, thanks for all you have done!

## ACKNOWLEDGMENTS

I appreciate the constructive criticism and recommendations of my advisor Dr. Tom McKee and the other members of my graduate committee: Dr. Steve Rutledge and Dr. Freeman Smith. Their advice helped guide my research and improve the final draft of this paper.

Thanks to Mr. John Kleist who provided valuable assistance with the computer work, and to Mrs. Odie Bliss whose hard work helped put this paper in its final form. Thanks also to Pat Kennedy and Dave Brunkow of the CHILL radar facility for the excellent job they did in gathering and processing the data used in this study. In addition, Doug Burks provided much assistance in using the algorithms needed to process the radar data.

Thanks most of all to the United States Air Force for providing the funding and opportunity for me to study at Colorado State University.

## TABLE OF CONTENTS

	<u>Page</u>
CHAPTER I. INTRODUCTION .....	1
CHAPTER II. DATA .....	4
A. Data Collection .....	4
1. Summer 1991 hydrology experiment .....	4
2. CSU-CHILL radar .....	5
3. Rain Gage Network .....	6
B. Weather Conditions .....	6
1. June 6, 1991 synoptic conditions .....	6
2. Severe weather reports .....	9
CHAPTER III. METHODS .....	11
A. Radar Rainfall Algorithm .....	11
1. Radar reflectivity factor-rainfall rate (Z-R) relations .....	11
2. Processing the radar data .....	15
3. Sources of error in radar rainfall estimates .....	16
B. Radar/Rain Gage Comparisons .....	19
1. Rain Gage Measurements .....	19
2. Methods of radar/gage comparison .....	20
CHAPTER IV. RESULTS FOR THE JUNE 6, 1991 DENVER THUNDERSTORM .....	22
A. Radar Rainfall Measurements .....	22
1. Temporal evolution of the rainfall pattern .....	22
2. Other Z-R relations .....	32
B. Hail Indicators .....	34
1. Reflectivity thresholds .....	37
2. Differential Reflectivity ( $Z_{DR}$ ) and Hail Detection Signal ( $H_{DR}$ ) .....	41
3. Difference Reflectivity ( $Z_{DP}$ ) .....	54
C. Summary .....	61
CHAPTER V. RESULTS FOR THE AUGUST 5, 1991 DENVER THUNDERSTORM .....	62
A. Storm Characteristics .....	62
B. Rainfall Measurements .....	62



1. Storm evolution .....	62
2. Other Z-R relations .....	71
C. Hail Indicators .....	73
1. Reflectivity thresholds .....	73
2. Differential Reflectivity ( $Z_{DR}$ ) and Hail Detection Signal ( $H_{DR}$ ) .....	73
3. Difference Reflectivity ( $Z_{DP}$ ) .....	74
D. Summary .....	75
 CHAPTER VI. CONCLUSIONS .....	 78
 CHAPTER VII. REFERENCES .....	 80

## CHAPTER I

### INTRODUCTION

Accurate measurements of thunderstorm rainfall are essential for providing timely guidance on flash flood potential. Precipitation measurements must be much closer together, both spatially and temporally, than those provided by the synoptic-scale observing network in order for this guidance to be useful. A dense array of automatic rain gages which transmit data to a central location meets these measurement requirements. The Denver Urban Drainage and Flood Control District (UDFCD) operates such a network, with 41 ALERT (Automated Local Evaluation in Real Time) gages in a 1296 km<sup>2</sup> area or 31.6 km<sup>2</sup> per gage. Although the Denver UDFCD gage network provides adequate data, it is expensive to maintain and only covers a limited area.

The use of weather radar to make rainfall estimates could help overcome the problems inherent in rain gage networks. A single radar provides high resolution data, in both space and time, over a very large area and is easier to maintain than dozens of gages. The accuracy of radar rainfall estimates is questionable in Colorado where hail is often present in large storms, which casts some doubt on the usefulness of these estimates. During the summer of 1991 Colorado State University's (CSU) Department of Atmospheric Science participated in an experiment which was intended, in part, to determine how useful radar measurements are in helping to estimate heavy rainfall from thunderstorms.

Weather radars have been used to estimate rainfall since the late 1940s, although technological hurdles such as assuring data accuracy and rapidly processing vast amounts of data have slowed the operational implementation of radars for this purpose. Atlas (1990) provides a historical overview, while Brandes and Wilson (1986) and Joss and Waldvogel (1990) give comprehensive surveys of the radar rainfall measurement field.

The most common method used to make radar rainfall estimates is based on the approximate relationship between the power returned to the radar and the rainfall rate. The power returned is expressed in terms of a reflectivity factor,  $Z$  ( $\text{mm}^6 \text{m}^{-3}$ ), while the rainfall rate,  $R$ , is in  $\text{mm/h}$ . These relations are of the form  $Z = AR^b$ , with  $A$  and  $b$  varying greatly depending on the region of the country, type of storm, and even the evolutionary phase of a single storm. Battan (1973) lists a total of 69 different  $Z$ - $R$  relations, each based on drop-size distributions measured in different locations and varying climates. No single  $Z$ - $R$  relation performs well in all areas or for all precipitation types, but improvement in radar rainfall estimates is possible by choosing an appropriate relation for the situation at hand.

Hailstones have been found to cause large errors in radar rainfall estimates because they scatter microwave radiation from the radar differently than liquid water and because they are larger than raindrops. Even small amounts of hail mixed with rain can result in reflectivity values considerably higher than those produced by rain alone. Hail is relatively common in Colorado, therefore its presence must be detected and accounted for when attempting radar rainfall estimates in this region.

The purpose of this study is to examine the performance of three  $Z$ - $R$  relations, as well as the effects of hail on radar rainfall measurements during two

Denver thunderstorms. These storms occurred on June 6 and August 5, 1991 and were observed by CSU's CHILL radar and the rain gage network of the Denver UDFCD during the summer 1991 hydrology experiment. The June 6 storm produced a peak rainfall amount of 43.7 mm (1.72 in), as well as 1.0" diameter hail during the 85 minute period studied. In contrast, no hail was observed at the surface during the August 5 storm, but rainfall amounts as high as 37.8 mm (1.49 in) were recorded during the 60 minute observational period. The June 6 storm is studied in the greatest detail because of the dramatic effect hail has on the radar rainfall estimates, while the August 5 storm provides a good example of a storm with no hail still producing large rainfall amounts.

## CHAPTER II

### DATA

#### A. Data Collection

##### 1. Summer 1991 hydrology experiment

During the summer of 1991 CSU's Department of Atmospheric Science participated in a hydrology experiment with a number of other agencies. Among the other participants were the Denver UDFCD and NOAA's Forecast Systems Laboratory (FSL). CSU provided data from the CSU-CHILL radar, UDFCD collected rainfall data from their network of gages, while FSL obtained data from the Mile High radar. The primary goal of the hydrology experiment was to collect precipitation data of a high spatial and temporal resolution, and to study the utility of using this data to predict runoff from thunderstorms in urban areas. This study focuses on the following question: how useful are radar measurements in helping to estimate heavy rainfall in thunderstorms? Rainfall rate data collected by the CHILL radar and simultaneous rain gage measurements from the UDFCD network are used to help answer this question. Storms producing 1.0 inch of rain or more over the rain gage network were sought. Data were collected on June 6, August 5, August 6, August 15, and August 28. This study will examine the June 6 event in detail and examine the August 5 event to a lesser extent.

## 2. CSU-CHILL radar

The CHILL is a 11 cm wavelength (S-band), pulsed Doppler weather radar with dual polarization capabilities. It is located 10 km east of Greeley, Colorado at an elevation of 1423 m. An S-band radar is preferred over a 5 cm (C-band) radar for rainfall measurements because attenuation from rain becomes significant at shorter wavelengths (Doviak, 1986).

During the June 6 storm data were collected between 1550 and 1826 MDT in a sector south of the radar where the most intense storms were occurring. Most of the sectors were between approximately 150 and 240 degrees azimuth, with several beginning at 190 degrees. Very little rain fell after 1715 MDT, therefore just the first 18 volume scans (1550–1715 MDT) were processed. The scans alternated between Plan Position Indicator (PPI) and Range Height Indicator (RHI) displays, with the PPI scans being used to derive rainfall amounts. Each PPI scan consisted of sweeps at 13 different elevations: 0.8, 1.6, 2.3, 3.0, 3.7, 4.5, 5.2, 7.6, 8.5, 9.5, 10.8, and 12.1 degrees. The PPI scans were made every 5 minutes and consisted of the following fields: returned power, radial velocity, spectral width, and normalized correlated power. Alternate PPI scans also included differential reflectivity data.

A scan at each elevation consisted of approximately 97 rays (0.96 degree beam width) out to a range of 180 km. The 150 m gate spacing yielded 1200 gates per ray or roughly 116,400 gates for each elevation scan. The radar data were stored on magnetic tape and converted to Universal Doppler Exchange Format (UF) by CSU-CHILL personnel.

### 3. Rain Gage Network

The Denver UDFCD operates a network of 60 tipping bucket rain gages situated throughout the drainage basins effecting the Denver metropolitan area (see Figure 2.1). This network is used to provide flash flood predictions for the large and small drainage basins in the region. The gages operate automatically and provide continuous data during rain events. The 36 by 36 km (1296 km<sup>2</sup>) area examined during the June 6 event contains 41 gages or 31.6 km<sup>2</sup> per gage. The gages range from 98.1 km (gage 1600) to 70.6 km (gage 1900) from the radar. Some portions of this region are much more densely instrumented. The Denver/Aurora vicinity (9-28 km west and 76-88 km south of the radar), contains 21 gages or 10.9 km<sup>2</sup> per gage.

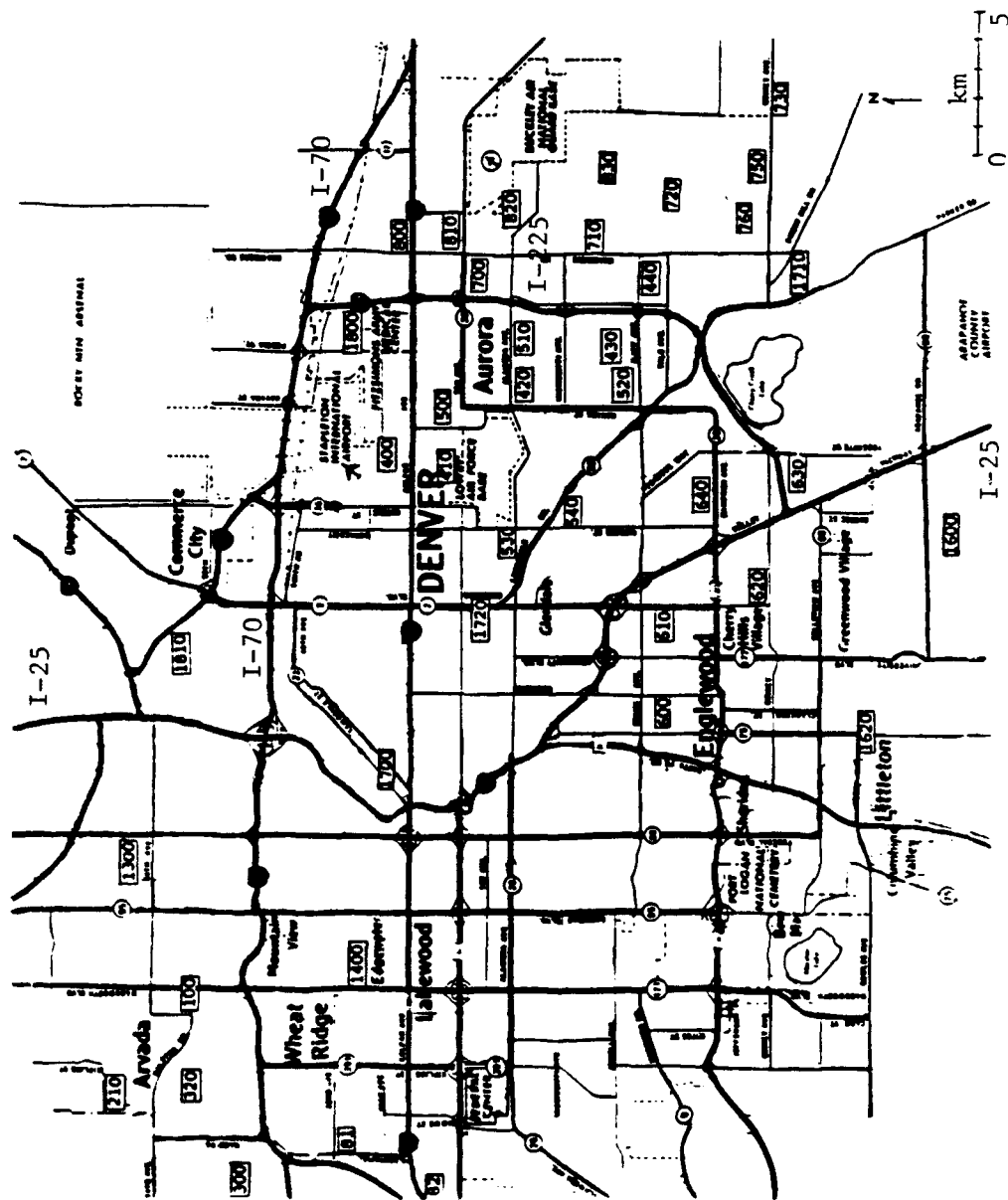
A somewhat smaller area was examined during the August 5 event, covering 936 km<sup>2</sup> with 33 gages (28.4 Km<sup>2</sup> per gage). As in the previous case, the Denver/Aurora vicinity, with its higher gage density, is examined.

### B. Weather Conditions

#### 1. June 6, 1991 synoptic conditions

Conditions on June 6 were favorable for the development of thunderstorms by early afternoon. The 1200 Z Denver sounding showed a conditionally unstable atmosphere with a Lifted Index (LI) of -1.0, an indication that thunderstorms were likely. Surface maps showed dewpoints across eastern Colorado near 55°F, with readings near 49°F along the Front Range. A low pressure system in extreme western Colorado created a weak pressure gradient across the state which induced southeasterly winds across eastern Colorado (Figure 2.2). These upslope winds advected additional moisture into the region. By 2100 Z a dryline was oriented north

Figure 2.1. Portion of the Denver UDFCD rain gage network used in this study. The rain gage numbers (in boxes) are referred to throughout this paper.





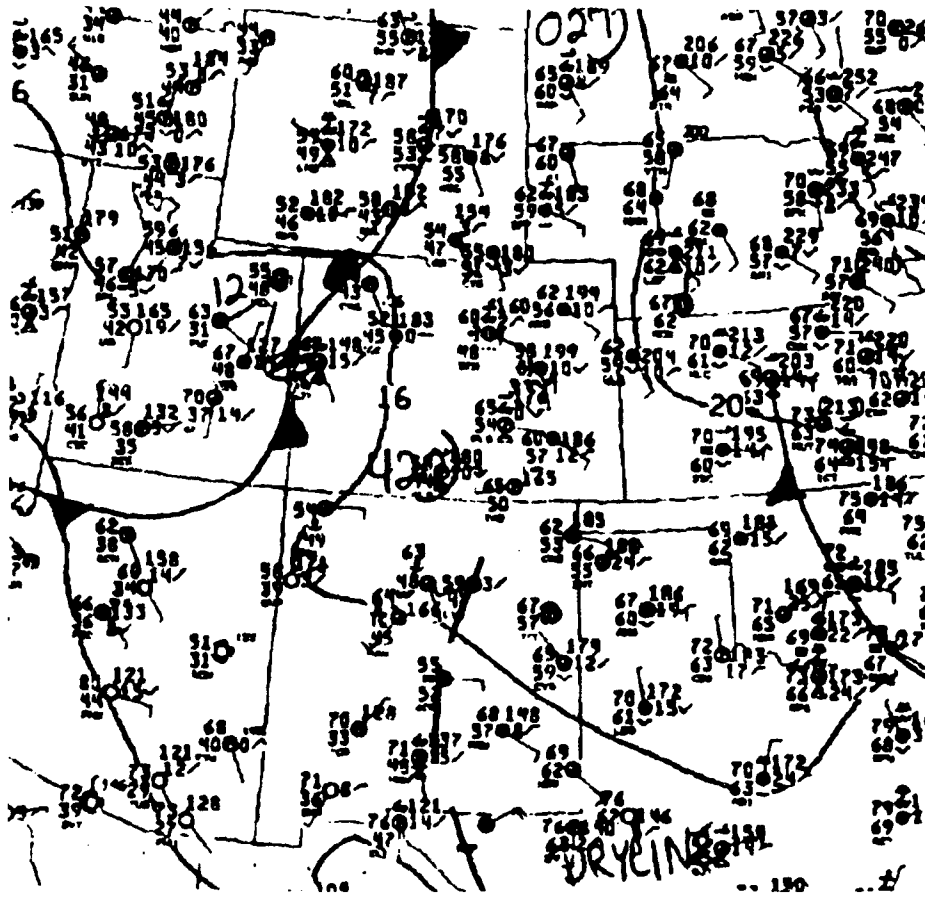


Figure 2.2. The 15Z surface chart for 6 June 1991.

to south along the Front Range, possibly acting as a trigger for thunderstorm activity. In addition, a weak vorticity maxima passed over eastern Colorado during the afternoon hours. Light upper level winds resulted in slow moving thunderstorm cells. Intense thunderstorms developed by mid-afternoon, with a report of flash flooding 40 miles southwest of Denver at 1520 MDT (NOAA, 1991).

## 2. Severe weather reports

Reports of severe weather were numerous in the Denver vicinity on the afternoon of June 6. The National Weather Service (NWS) issued an urban and small stream flood advisory for the Denver metropolitan area at 1605 MDT. This advisory was updated to focus on the Aurora area at 1630 MDT:

"Massive street flooding in SE Aurora ... Rainfall reports of over an 1.5 inches per hour have been received from amateur radio operators and the public ... The heavy rain is accompanied by pea to marble size hail and numerous funnel clouds..."

The following summary, taken from Storm Data (NOAA, 1991), provides further information on the nature of this storm:

"Thunderstorms moved through Aurora and dropped hail up to 1.00" in parts of the city ... Very heavy rain in excess of 1.00 inch in 30 to 60 minutes flooded roads in Aurora. Water was reported hood-deep 9 miles east of Denver ... Early damage surveys placed hail and water damage to automobiles and houses at \$350,000."

Storm Data also reported the following times of occurrence in Aurora: flash flooding at 1649 and 1716 MDT, 1.00 inch hail at 1609 and 1615 MDT, and 0.75 inch hail at 1626 and 1716 MDT. In addition, weak (F0 and F1) tornadoes were reported

east of Buckley Air National Guard Base (ANGB) at 1621 and 1640 MDT,  
respectively.

CHAPTER III  
METHODS

A. Radar Rainfall Algorithm

1. Radar reflectivity factor-rainfall rate (Z-R) relations

Of the many methods available to make radar rainfall measurements, making use of the relationship between the power returned to the radar expressed in terms of reflectivity factor,  $Z$  ( $\text{mm}^6 \text{ m}^{-3}$ ), and the rainfall rate,  $R$  ( $\text{mm h}^{-1}$ ), is the most common. Derivation of Z-R relationships is based upon the radar equation, basic cloud physics considerations, and several assumptions (see Brandes and Wilson, 1986 and Burgess and Ray, 1986). The average power per unit volume  $\Delta V$  returned to the radar is given by the sixth power of drop diameter summed over all the drops in  $\Delta V$ . Therefore  $Z$  is related to the dropsize distribution:

$$Z = \frac{1}{\Delta V} \sum_{i=1}^N D_i^6 = \int_0^{\infty} N(D) D^6 dD \quad (1)$$

where  $N(D)$  is the number of drops of diameter  $D$ . Raindrop size distributions are generally exponential and can be expressed in the form given by Marshall and Palmer (1948):

$$N(D) = N_0 e^{-\Lambda D} \quad (2)$$

Clearly there are departures from this simple form, which was derived for stratiform rain events.  $N_0$  and  $\Lambda$  vary significantly from storm to storm, leading to difficulties in the Z-R method. Marshall and Palmer found  $N_0$  to be  $8000 \text{ m}^{-3} \text{ mm}^{-1}$  and  $\Lambda = 4.1R^{-0.21}$ . When the vertical wind speed is zero, often a poor assumption in thunderstorms, the rainfall rate is given by:

$$R = \frac{\pi \rho}{6} \int_0^{\infty} D^3 V_t(D) N(D) d(D), \quad (3)$$

where  $\rho$  is the density of water and  $V_t(D)$  is the droplet terminal velocity. Work by Spilhaus (1948) shows that  $V_t = 1400D^{0.5}$  (cgs units); other forms are discussed by Doviak and Zrnić (1984). Equations (1), (2), and (3) are combined to yield a relation of the form:

$$Z = AR^b. \quad (4)$$

Because dropsize distributions are seldom known accurately and vertical velocities are often significant, the above relation is not unique. Table 3.1 summarizes the three relations used in this study, while Figure 3.1 provides a plot of the relations.

MP is based on a Marshall-Palmer dropsize distribution and is best suited for stratiform rain situations. NR performs adequately across a wide range of locations and weather conditions, therefore it has been chosen to be the default Z-R relation for NEXRAD (NEXRAD, 1982 and Ahnert et al., 1983). Since NR was developed in Florida (Woodley and Herndon, 1970), it does not appear to be a good a priori choice for a dry climate like Colorado's. CO was developed by Kelsch (1989) in an attempt to account for evaporation below cloud base, especially in light rain. This

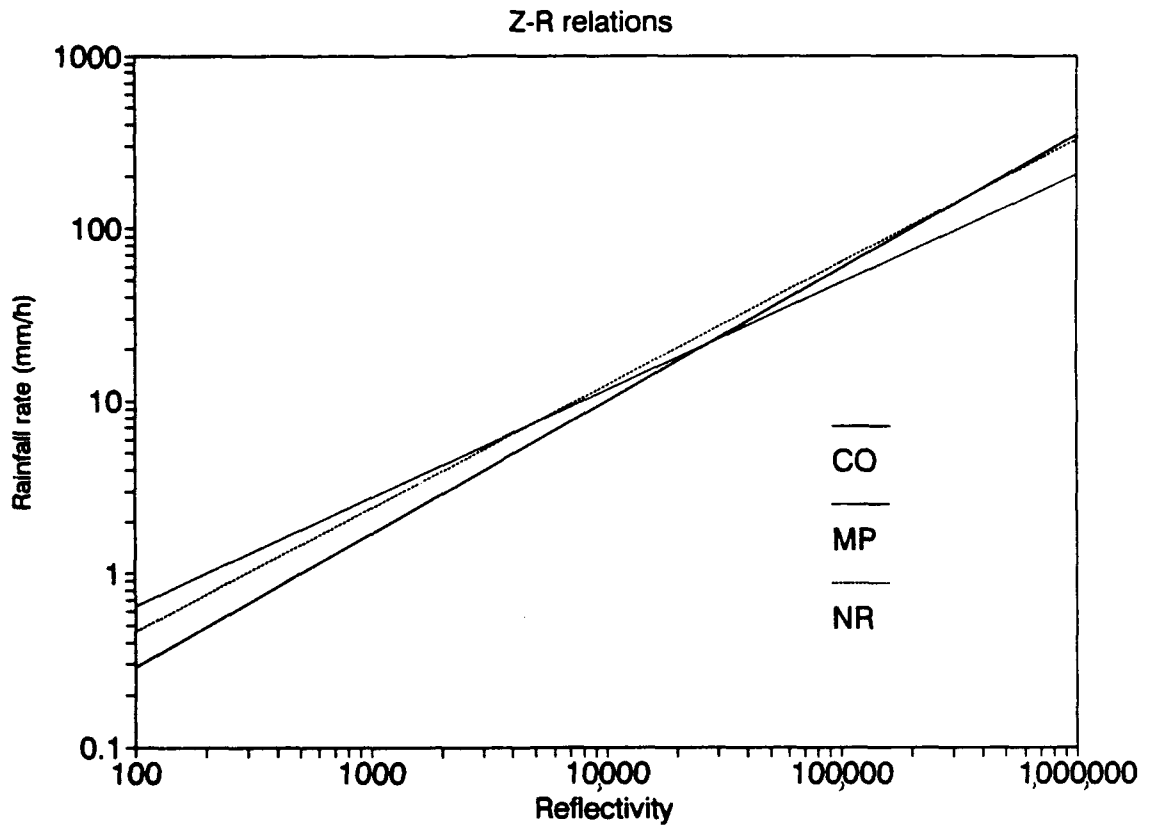


Figure 3.1. Plot of the three Z-R relations used in this study: CO ( $Z = 500R^{1.3}$ , MP ( $Z = 200R^{1.6}$ ), and NR ( $Z = 300R^{1.4}$ ). Reflectivity is given in linear units ( $\text{mm}^6/\text{m}^3$ ).

Table 3.1

## Z-R relations used in this study.

<u>Relation</u>	<u>Symbol</u>	<u>Rainrate (mm/h) for:</u>		<u>Comments</u>
		<u>55 dBZ</u>	<u>30 dBZ</u>	
$Z = 500R^{1.3}$	CO	142.3	1.7	Developed for Colorado to account for evaporation (Kelsch, 1989).
$Z = 200R^{1.6}$	MP	99.8	2.7	Based on a Marshall-Palmer dropsize distribution. Good for stratiform rain events.
$Z = 300R^{1.4}$	NR	143.7	2.4	Used by Woodley and Herndon (1970) for thunderstorms in Florida. NEXRAD default.

study will use all three relations to some degree, but will concentrate on the CO relation.

Obviously the choice of "best" Z-R relation is as varied as the drop size distribution, vertical wind structure, and other physical attributes of the storm in question. The appropriate Z-R relation will vary from region to region, from day to day, and even between different sections and developmental stages of the same storm. In general, the coefficient in (4) increases and the exponent decreases with the intensity of convection (Brandes and Wilson, 1986). Table 3.2 (after Brandes and Wilson, 1979) shows other processes which lead to variations in Z-R relations.

Table 3.2

## Effects of various processes on Z-R relations

<u>Process</u>	Change in $Z = AR^b$		<u>Probable effect on radar rainfall estimate</u>
	<u>A</u>	<u>b</u>	
Evaporation	Increase	Decrease	Overestimate
Updrafts	Increase	Decrease	Overestimate
Downdrafts	Decrease	Increase	Underestimate

## 2. Processing the radar data

Each volume scan, approximately 3.5 minutes of data, is in a separate file of roughly 10 megabytes each. The data were first interpolated to Cartesian coordinates using SPRINT (Sorted Position Radar Interpolation) (Mohr et al., 1981). The user must specify the size and location of the grid by entering the minimum and maximum x and y distances from the radar. The height of the plane and grid resolution are also input.

The grid used for the June 6 storm extends from 60 to 96 km south and 9 to 45 km west of the radar, with a 1 km grid spacing. The 3.5 km MSL (1.9 km AGL) level was chosen because it was the lowest Constant Altitude PPI (CAPPI) which included nearly all of the gages in the grid. As will be discussed later, sampling a region close to the surface helps reduce the effects of evaporation and wind drift on precipitation estimates. Several volume scans from June 6 are missing a portion of the 3.5 km level (volumes 1, 6, 13, 23, 28, 33, and 38) because the 0.8 degree sweep did not proceed far enough eastward. Information from 4.5 km is used to fill in these missing areas.



The grid used to study the August 5 event is slightly smaller in the x-direction, starting 35 km west of the radar. In this case the 3.0 km MSL CAPPI could be used to provide complete coverage of the study area. There were no problems with missing sectors during this event.

After the reflectivity data in each file has been interpolated to the 3.5 km MSL plane, computation of rainfall rates can begin. A FORTRAN program was used to make the necessary computations and to compare the radar estimates with the rain gage amounts. The user inputs the desired Z-R relation, time period of interest, and reflectivity threshold and the program performs the accumulations at each pixel. The precipitation amount calculated for the pixel nearest each gage is used to compare the radar estimates with the gage amounts.

### 3. Sources of error in radar rainfall estimates

Numerous potential sources of error exist in the process of generating radar rainfall estimates. One source of error, already touched on, is the use of an improper Z-R relation for the situation at hand. A relation found to perform well during a stratiform rain event in Seattle would probably not display the same success during a Colorado thunderstorm. Although improvements in radar rain estimates can be made by selecting the Z-R relation based on storm type, large errors still remain. For example, Jones (1966) selected the Z-R relation based on the storm type and was able to reduce radar errors from 62% to 43%.

Ground clutter (topography, buildings, trees, etc.) can cause partial screening of the radar beam, resulting in shadows in the radar rain pattern. Ground clutter may also produce false echoes in areas where no rain is actually falling. Examination

of topographical maps shows that screening between CHILL and the area observed is not a problem. The bottom of the 0.8 degree beam is at an elevation of about 2300 m in the Denver area, roughly 700 m above the ground.

Temperature inversions may cause anomalous propagation or ducting of the radar beam. This phenomenon may cause false echoes to appear or actual rain regions to be missed. Strong low-level inversions, such as those caused by the cold outflow from a thunderstorm, can cause ducting or anomalous propagation to occur. Examination of temperature soundings and radar echo displays on both days indicates that ducting was not likely during the times of observation. The CHILL personnel process the radar data in an attempt to remove clutter from aircraft and tall buildings.

Another source of error is the inaccurate measurement of radar reflectivity factor  $Z$ . Equipment calibration problems occasionally may lead to small errors in  $Z$ . The independent motions of the target particles can also cause measurement errors, even after averaging in space and time is used to reduce this effect. As the distance from the radar increases, the beam illuminates increasingly larger volumes. Partial beam filling may result, in which the echo occupies just a portion of the sample volume. This generally results in rainrate underestimates (Wilson, 1975).

Even if measurements of  $Z$  and the  $Z$ - $R$  relation used are perfect, meteorological processes occurring below the radar beam can still lead to large errors in radar rainfall estimates. Evaporation below the level sampled by the radar can result in large overestimates of the rain amounts reaching the ground. The 3.5 km CAPPI used for the 6 June event is roughly 1.9 km above the ground, significant evaporation can occur in this distance. Strong winds can cause drift of precipitation

below the radar beam, therefore measurements at the beam level are not always applicable on the ground directly below. Large reflectivity gradients oriented perpendicular to the wind direction will intensify this effect.

The presence of ice within the radar sample volume introduces other uncertainties. Because the index of refraction for water droplets is roughly five times greater than that for similarly-sized ice particles, droplets scatter more energy back toward the radar and are therefore more easily detected. This explains why snow is often difficult to detect with weaker radars like the WSR-57. These differences in index of refraction may also be used to explain the radar bright band, a zone of enhanced reflectivity often detected by a radar just below the 0°C level in stratiform precipitation. As snow falls below the 0°C level and begins to melt, its reflectivity increases sharply. This is because water has a dielectric constant roughly four times that of ice, therefore, more power is returned to the radar. This results in a distinctive band of high reflectivity values just below the 0°C level. As the melting is completed, the resulting water droplets are somewhat smaller and fall more rapidly, thus lowering the particle concentration, causing a further reduction in Z. The unrepresentatively high reflectivity values of the bright band can lead to large overestimates in radar rainfall rates.

Hail can also cause the radar to overestimate rainfall rates. The reflectivity of a hailshaft can be very complex because it depends on several factors: The wetness of the hail, the hail size distribution, and the mean hailstone diameter, to name a few. In general hail results in a large increase in the reflectivity, often leading to overestimates by the radar (Battan, 1973; Ulbrich and Atlas, 1982;

Lipshutz et al., 1989; and Aydin et al., 1990). The effects of hail on radar rainfall measurements are discussed in detail later in this thesis.

Time and space sampling by the radar also leads to errors in many cases. In this study the CSU-CHILL radar sampled a radar volume approximately every 5 minutes. Fluctuations in rainfall rate can occur on much shorter time scales and may be completely missed by the radar. A rain gage samples continuously and therefore will record any variations in rainfall rate, this acts to decorrelate point gage/radar comparisons.

## B. Radar/Rain Gage Comparisons

### 1. Rain Gage Measurements

Rain gage measurements, whether they are from tipping-bucket type gages or standard gages, should not be assumed to be completely accurate. Sources of error include turbulent airflow near the gage, evaporation, adhesion of drops to the gage sides, and water splashing out of the gage. Except for airflow around the gage, these processes are thought to account for underestimates of no more than 2% (Dahlstrom, 1973). Thunderstorm rainfall measured by identical gages within 2 m of each other revealed differences averaging 9% (Woodley et al., 1975). As air is diverted around the gage, particles that would have been caught are deflected and carried away. This process probably accounts for most of the gage measurement error. Larson and Peck (1974) examined several independent studies and found undercatchment to increase with wind speed. They report 12% and 19% deficiencies for windspeeds of 5 m/s and 10 m/s, respectively. Hail may also cause measurement problems in gages. Melting

hailstones in an automatic rain gage could give the appearance of light rain falling after the time at which the rain actually ceased.

The Denver UDFCD uses 12" diameter gages which funnel precipitation into an internal tipping bucket. The bucket tips and records each time 1 mm of rain accumulates. The lip of each gage is 3 m above the ground and not screened from the wind, so the wind effects mentioned above probably contribute to error. Each gage has a clear view of the sky from 45 degrees above the horizon, reducing blockage from trees or buildings. The funnel opening has a screen to keep out all but the smallest hailstones. This screen probably prevents inaccuracies due to melting hail, but conceivably hailstones could come to rest on the screen and melt later (Kevin Stewart of the Denver UDFCD, personal communication). While it is clear that rain gages do not measure rainfall with complete precision, for the purpose of this study the Denver UDFCD gages are used as ground truth and thus are considered to be 100% accurate.

## 2. Methods of radar/gage comparison

Several methods are used to compare radar rainfall estimates, RA, and gage rainfall measurements, G. Those used in this study are listed below.

$$\text{difference} = RA - G \quad (5)$$

$$\text{percent difference} = 100\%(RA - G)/G \quad (6)$$

$$\text{gage-to-radar ratio} = \frac{G}{RA} \quad (7)$$

These are used to make comparisons at individual gages, as well as in an average sense for all the gages. A simple difference (5) is useful in cases when  $G = 0$ , this is especially common over short time periods. In these cases (6) and (7) are useless. Of course (5) also has problems. A difference of 5 mm will obviously be significant for a gage measurement of 2 mm, but this same difference will indicate an accurate radar estimate if the gage reports 25 mm, for example. Equations (6) and (7) compare gage and radar amounts in a relative sense, thereby avoiding this problem. On the other hand, (5) also has its advantages. A  $G/RA$  ratio of 1 mm/4 mm for location X and  $G/RA = 10 \text{ mm}/40 \text{ mm}$  at location Y would both equal 0.25, but the overestimate at Y would certainly be more significant from a forecasting/weather advisory standpoint. A simple difference is preferable in this instance. Because of the advantages/disadvantages inherent in each, all three will be used.

## CHAPTER IV

### RESULTS FOR THE JUNE 6, 1991 DENVER THUNDERSTORM

#### A. Radar Rainfall Measurements

##### 1. Temporal evolution of the rainfall pattern

All radar rainfall estimates in this section are made using  $Z = 500R^{1.3}$ . Refer to Figure 2.1 for gage locations.

During the first 10 minutes of the storm monitored (1550-1600 MDT) the heaviest rain fell just south of Buckley ANGB (gage 830) where 11.2 mm was recorded (Figure 4.1a). Radar estimates showed the heaviest rain fell in the same area (Figure 4.1b), but the amounts were overestimated, with 24.3 mm indicated at gage 830.

Between 1600 and 1615 MDT the area of maximum rain accumulation shifted 4 km to the west, with 14.2 mm recorded at gage 440 (Figure 4.2a). Once again the radar rain estimates peaked in the same area, but were much greater in magnitude (Figure 4.2b). The CSU-CHILL estimated 44.5 mm at gage 440, an error of 30.3 mm (1.2 in) in just 15 minutes. The radar estimate for gage 710, 2.0 km to the northeast, was even worse with an error of 37.3 mm (1.47 in). A secondary maxima of 14.2 mm was indicated by the radar 3 km northwest of Cherry Creek Reservoir (gage 640), but the gage only showed 2.0 mm. Of the 16 gages recording precipitation during this period, rainfall was overestimated by the radar at 15 of them.

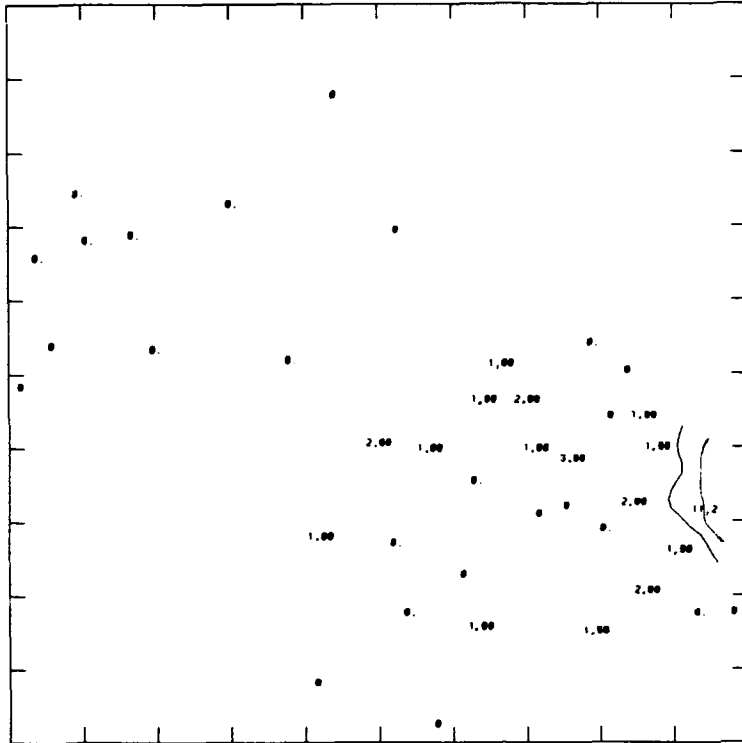


Figure 4.1a.

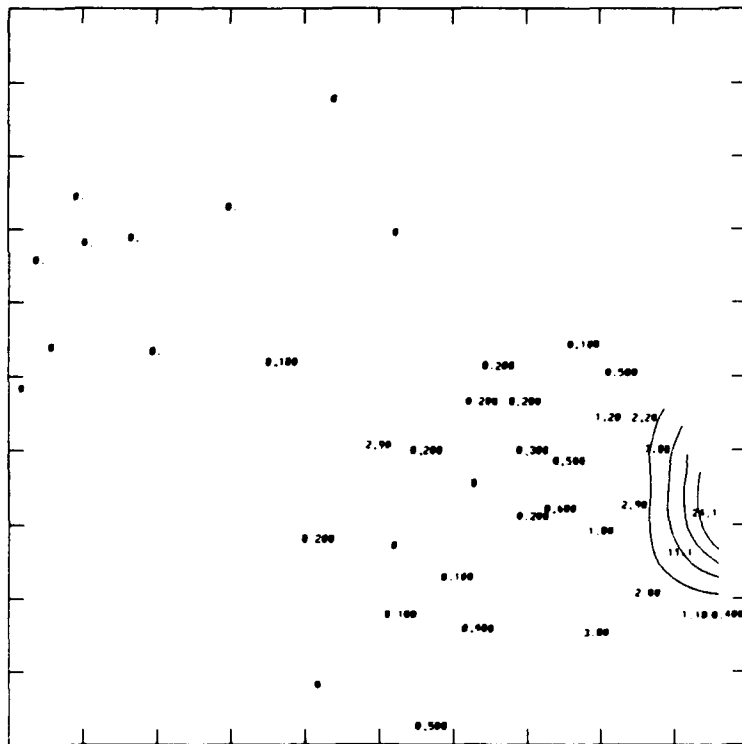


Figure 4.1b.

Figure 4.1. Rainfall (mm) for 1550-1600 MDT determined from a) raingages, and b) radar using  $Z = 500R^{1.3}$  and no threshold.



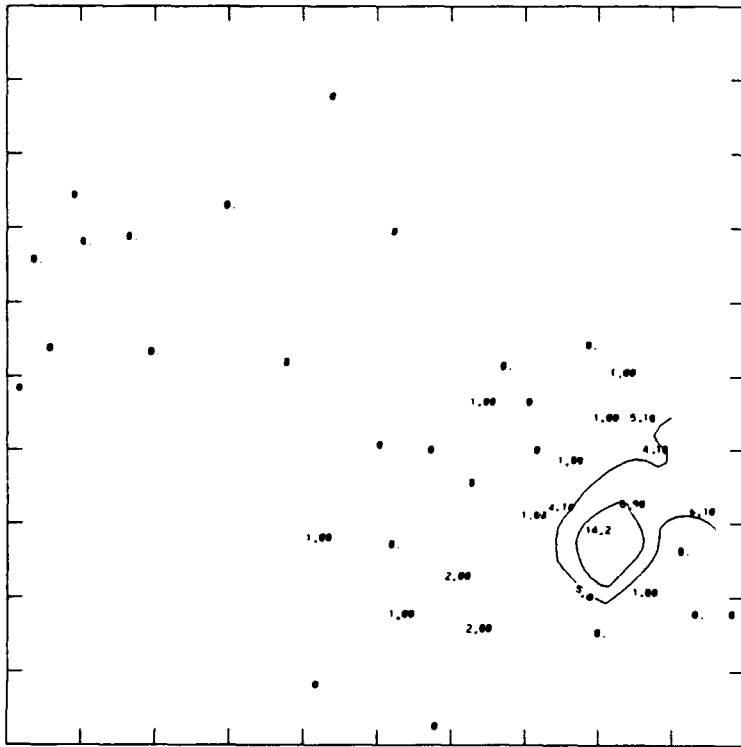


Figure 4.2a.

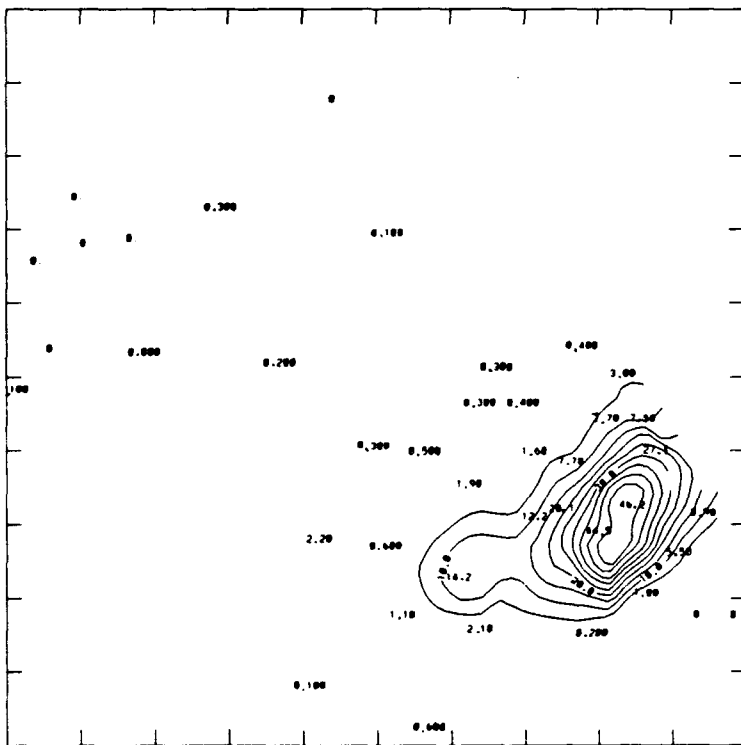


Figure 4.2b.

Figure 4.2. Same as Fig. 4.1, but for 1600-1615 MDT.

Between 1615 and 1630 MDT, the area of peak rainfall shifted 5.0 km to the north, to just west of Buckley ANGB (Figure 4.3a). Gages 700, 810, and 820 recorded 18.3, 17.3, and 18.0 mm, respectively. The radar estimates showed a rainfall peak in the same area, with much smaller errors than previous periods. Radar estimates for gages 700, 810, and 820 are 20.2, 15.6, and 27.9 mm, respectively (Figure 4.3b). The secondary radar rainfall maxima noted in the previous period moved 4.5 km to the north and intensified. There was no indication of this maxima in the rain gage measurements. This feature was centered 1.0 km south of Lowry AFB, with an estimate of 18.3 mm (0.72 in) at gage 540; the actual amount was only 3.0 mm. Just to the northwest, gage 530 measured 1.0 mm, while the radar estimated 8.3 mm of rain. Twelve out of the 16 gages recording 2.0 mm of rain or more were overestimated.

During the next 15 minute period (1630-1645 MDT) the rainfall maxima west of Buckley ANGB weakened significantly. Gages 700, 810, and 820 now indicate 10.2, 10.2, and 7.1 mm, respectively (Figure 4.4a). This collapse was also indicated in the radar estimates, which were still somewhat high (Figure 4.4b). The area of peak rainfall was now centered just to the east of Lowry AFB, where gage 420 reported 17.3 mm (0.68 in). Although the CSU-CHILL overestimated this gage by 19.8% (3.4 mm), larger errors occurred south of Lowry where the radar maximum was located. The radar estimate for gage 540 was 53.6 mm, while the gage recorded 14.2 mm. This is an overestimate of 39.4 mm (1.55 in) or 277%. The radar estimate for nearby gage 530 was 11.2 mm (0.44 in) too high. Twelve out of the 19 gages recording at least 2.0 mm of rain were overestimated by the radar.

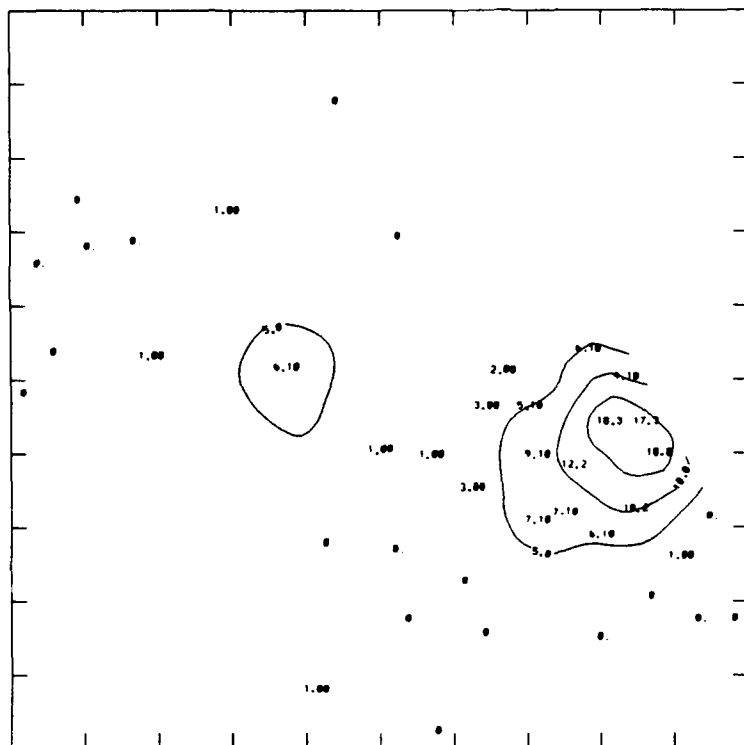


Figure 4.3a.

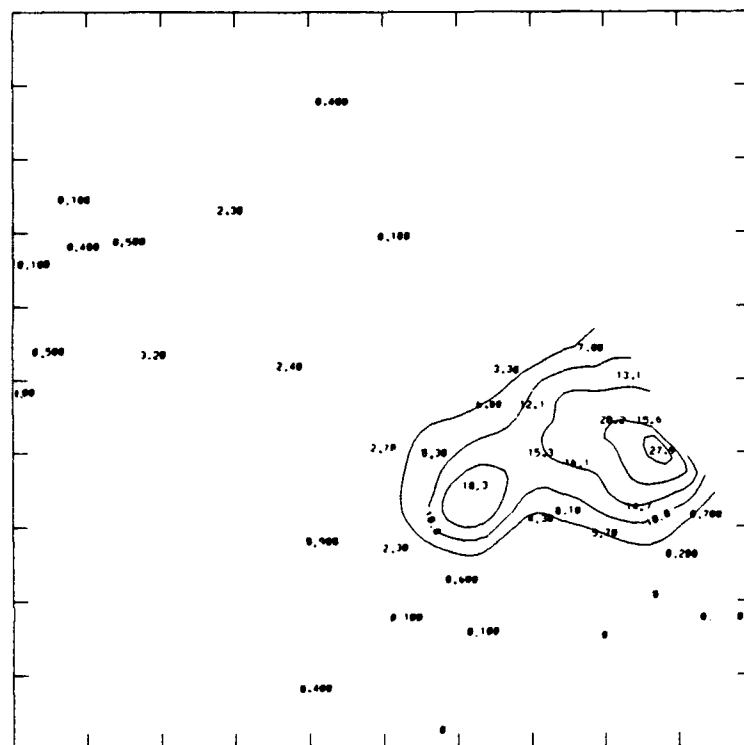


Figure 4.3b.

Figure 4.3. Same as Fig. 4.1, but for 1615-1630 MDT.

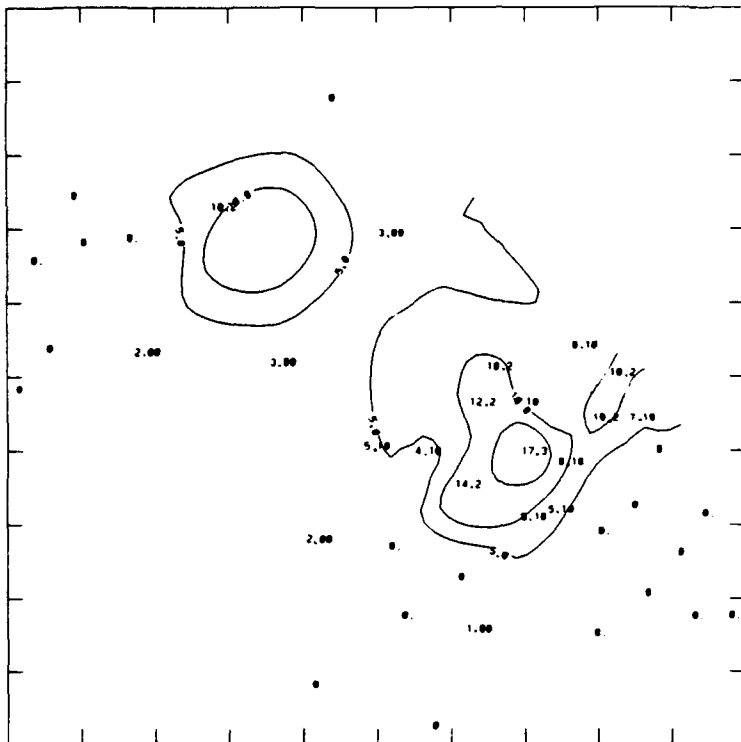


Figure 4.4a.

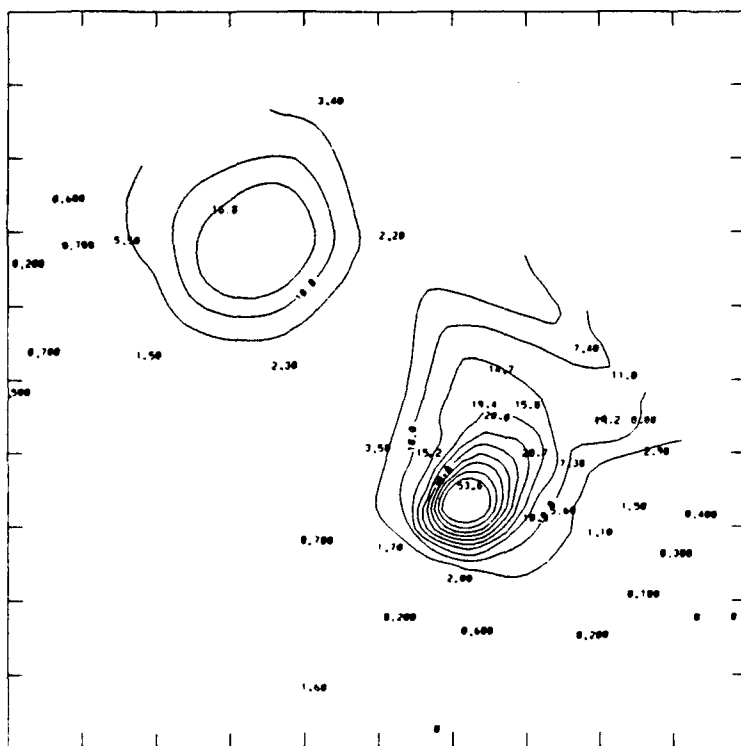


Figure 4.4b.

Figure 4.4. Same as Fig. 4.1, but for 1630-1645 MDT.

From 1645 to 1700 MDT the area of heaviest rain remained in the same general location, but expanded somewhat to the north and south (Figure 4.5a). Gages 500 and 520 recorded 16.0 mm (0.63 in) and 15.2 mm (0.60 in), respectively. These gages helped define a pattern with a double maxima, one centered just northeast of Lowry AFB and another 6 km to the south. The radar rainfall estimates gave a similar pattern, except the southern maxima was shifted 3.5 km to the northwest (Figure 4.5b). The most striking difference appeared in the magnitude of the radar rainfall estimates, several of which were less than the gage amounts during this period. The radar estimate was 9.2 mm (0.36 in) too low for gage 520. Of gages receiving 2.0 mm of rain or more, 17 out of 22 were underestimated by the radar.

During the last period (1700-1715 MDT) the storm appeared to be in the decay stage, with gage 510 in Aurora reporting the maximum amount of 7.1 mm (Figure 4.6a). As in the previous period, the radar underestimates most of the gage amounts (Figure 4.6b): all 16 gages receiving 2.0 mm or more were underestimated by the radar.

As might be expected, the storm total (1550-1715 MDT) plots show large differences, primarily in magnitude (see Figures 4.7a and b). The Aurora vicinity received the heaviest rainfall with gages 420, 510, and 700 each recording just over 40.0 mm (1.57 in). The radar rainfall amounts for these gages were within 15% of the actual measurements, but estimates for gages to the southeast and southwest displayed large errors. Gage 540 (1 km south of Lowry AFB) received 29.2 mm, but the radar estimated 88.0 mm, giving an error of 58.8 mm (2.31 in). Gage 530 recorded 9.1 mm (0.36 in), while the radar estimate was 28.3 mm (1.11 in): an error of 19.2 mm (0.76 in). These two radar estimates helped define an intense maxima

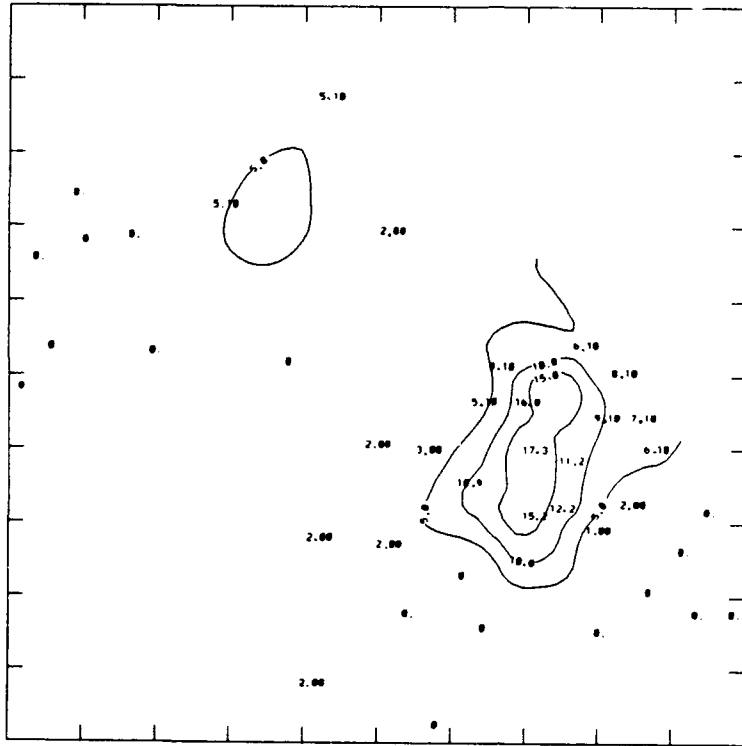


Figure 4.5a.

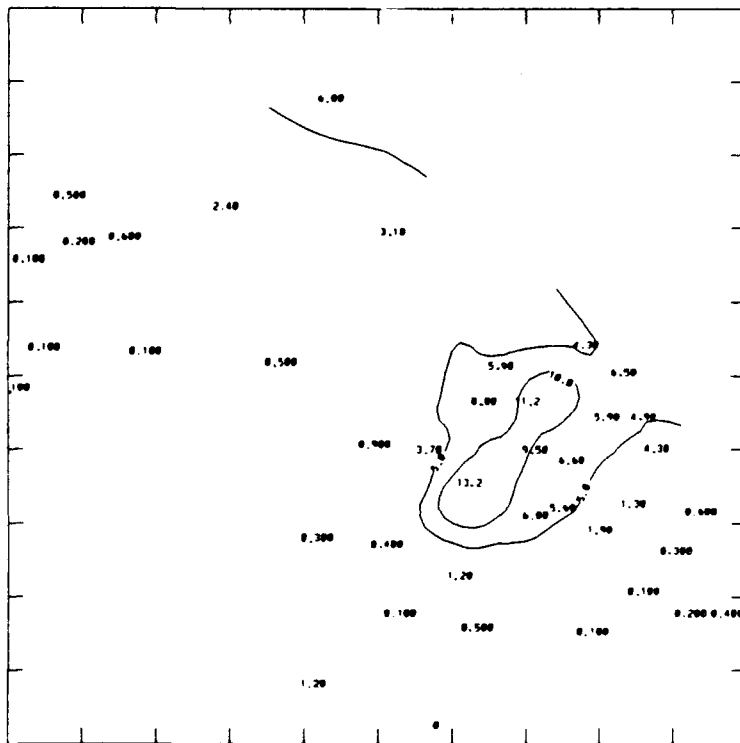


Figure 4.5b.

Figure 4.5. Same as Fig. 4.1, but for 1645-1700 MDT.

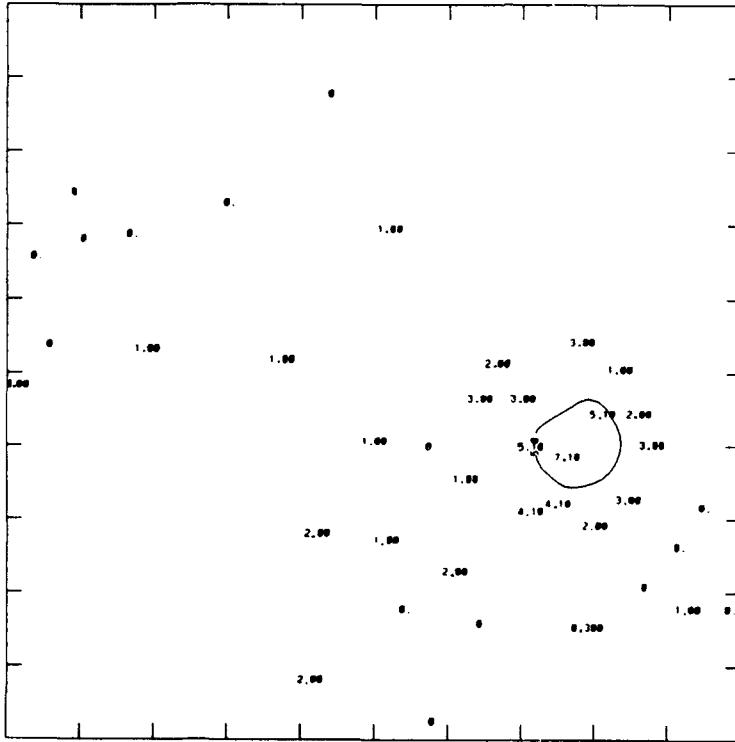


Figure 4.6a.

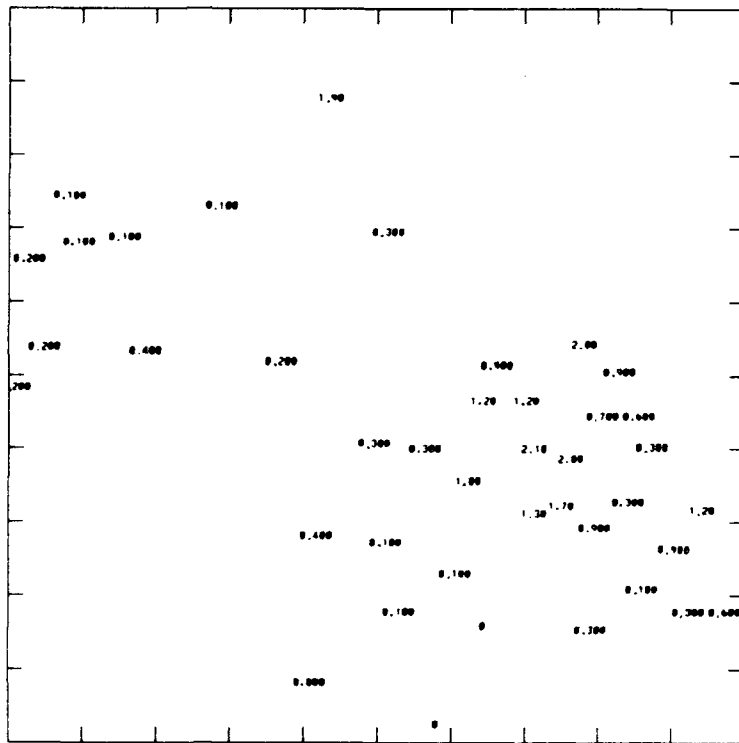


Figure 4.6b.

Figure 4.6. Same as Fig. 4.1, but for 1700-1715 MDT.

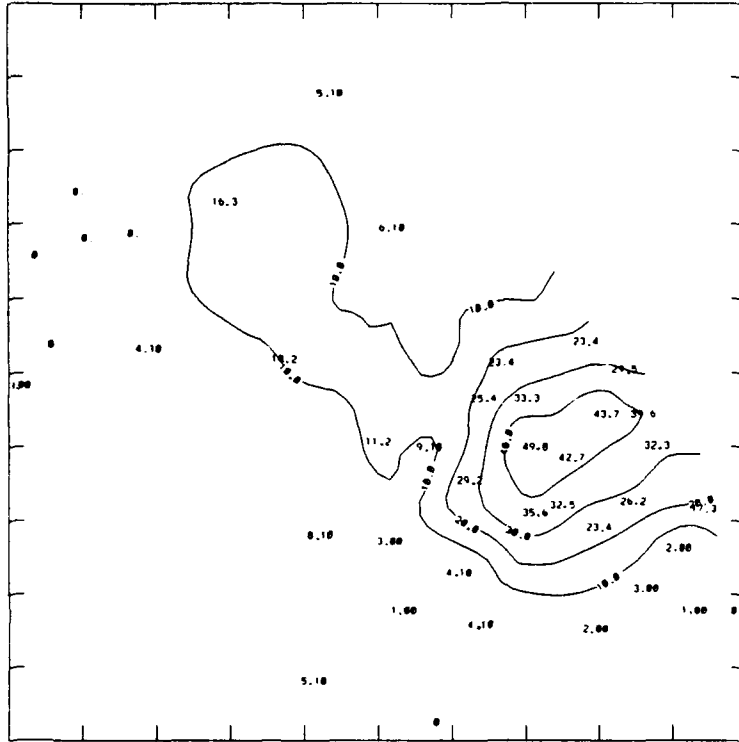


Figure 4.7a.

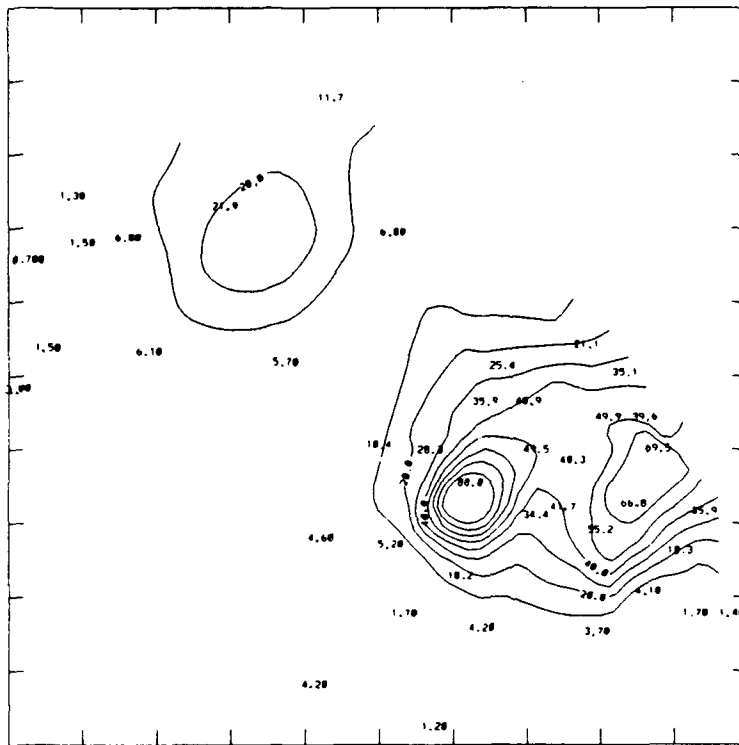


Figure 4.7b.

Figure 4.7. Same as Fig. 4.1, but for the entire storm, 1550-1715 MDT.



which does not exist in the gage rainfall plot. Over 90% of the overestimation at these gages occurred during the third and fourth periods (1615-1645 MDT). A second maxima was indicated by the radar 8.0 km east of the first, just to the west of Buckley ANGB. Gages 440, 710, and 820 were overestimated by 31.8, 40.6, and 37.3 mm, respectively. Most of the error resulted from large overestimates between 1600 and 1615 MDT.

Figures 4.8a and 4.8b illustrate the changing pattern in the radar precipitation estimates as the storm evolved. The radar overestimated rainfall the most during the first four periods (1550-1645 MDT), but this trend changed dramatically during the last two periods. This change appeared to be associated with the decay of the storm. Radar rain totals were higher than gage amounts at 31 of the 41 gages, with the largest underestimate being 4.4 mm (0.17 in) at gage 1700. Radar estimates were too high by more than 25.4 mm (1.0 in) at four gages and by at least 12.7 mm (0.5 in) at four other gages during the 85 minute study period. Clearly the use of this information in making urban flood forecasts or advisories could result in false alarms and overestimates of the flood potential.

## 2. Other Z-R relations

As discussed in Chapter 3, a large number of Z-R relations exist for different conditions and locations. This section will examine the performance of two other common relations:  $Z = 300R^{1.4}$  (NR) and  $Z = 200R^{1.6}$  (MP). Refer to Chapter 3 for further discussion of these relations.

NR was chosen because it is the default relation for NEXRAD. The radar rainfall pattern produced with this relation is very similar to that produced using

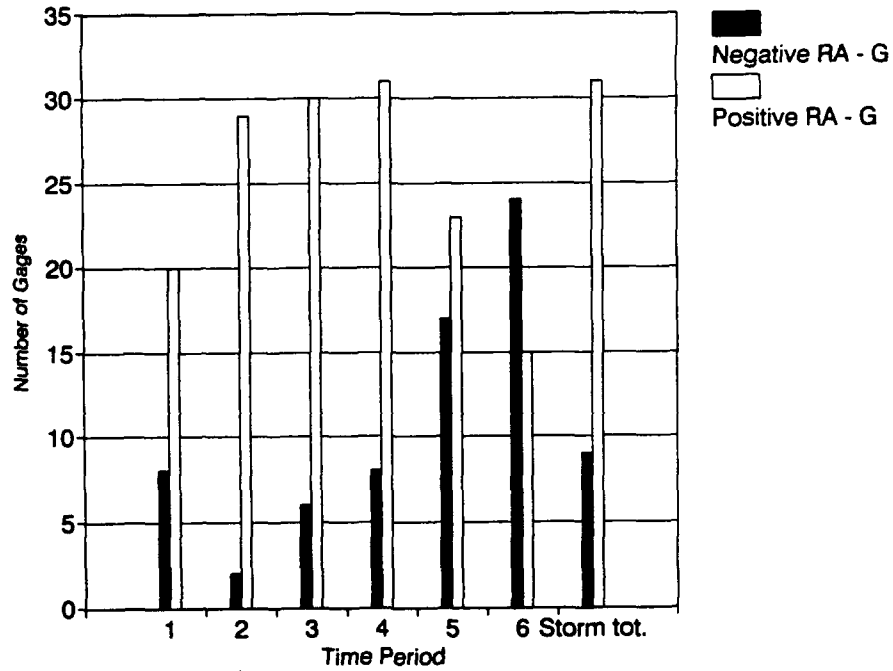


Figure 4.8a. Number of gages overestimated and underestimated by the radar during periods 1 (1550-1600), 2 (1600-1615), 3 (1615-1630), 4 (1630-1645), 5 (1645-1700), 6 (1700-1715), and the entire storm (1550-1715). All times MDT.

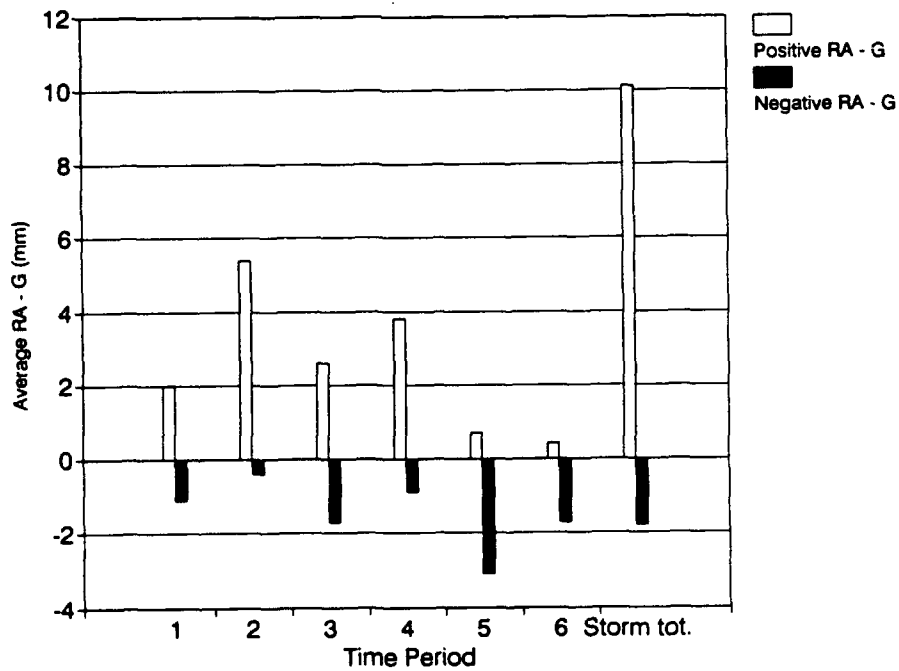


Figure 4.8b. Average difference (RA - G) in mm during the same periods as above.

$Z = 500R^{1.3}$  (CO), but rainfall estimates are slightly higher at each gage (see Figure 4.9). NR was developed for a humid climate, therefore it does not adequately take evaporation into account, resulting in overestimates in a generally less humid region like Colorado. This effect is most noticeable for low rainrates. Figure 4.11 shows  $G/RA$  for each relation in three different rainfall categories: light (gage  $\leq 5.0$  mm), moderate (gage 5.1–24.9 mm), and heavy (gage  $\geq 25.0$  mm). The light rainfall category is overestimated badly by each relation, probably a result of evaporation below the level sampled by the radar. The CO relation is intended to help reduce error due to evaporation and appears to accomplish this goal in this case, but problems obviously remain.

MP results in much lower precipitation estimates at each gage (Figure 4.10), with the estimate for gage 540 being 26.2 mm (1.02 in) lower than for the CO relation. Figure 4.11 shows that rainfall estimates are much better in the moderate and heavy categories for each relation, with MP performing the best of all. This seems surprising at first since MP was derived for stratiform rain events, not high-based Colorado thunderstorms. Evidence suggests, however, that hail may be causing unusually high reflectivity values in the storm core. This results in overestimation of rainfall, an effect which is less significant in MP since it produces lower rainrates than CO or NR at high  $Z$  values. Evidence for the presence of hail will be presented in the next section of this chapter.

## B. Hail Indicators

The presence of hail in a thunderstorm can lead to errors in radar rainfall estimates. For this reason hail should be accounted for, if possible, in order to

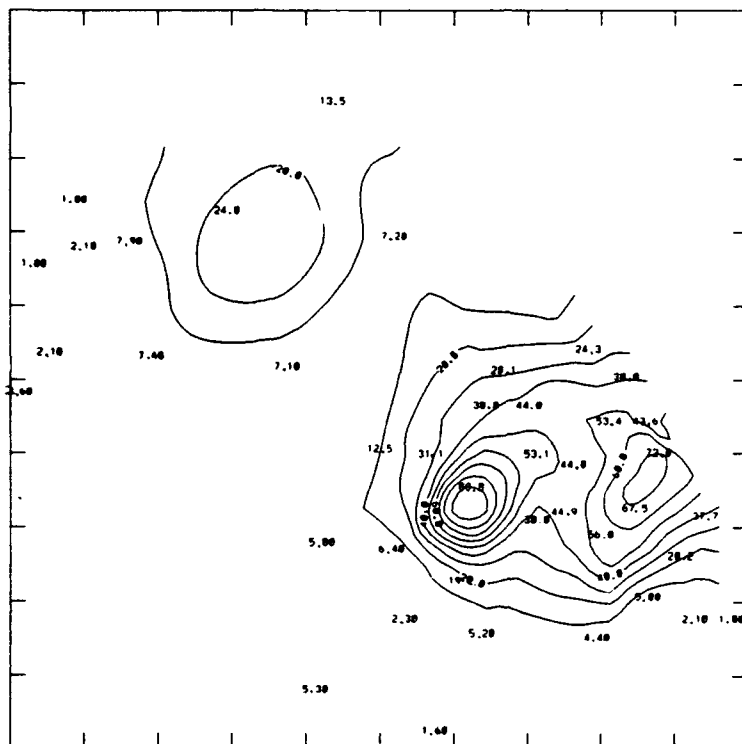


Figure 4.9. Radar rainfall estimated using  $Z = 300R^{1.4}$  and no threshold for 1550-1715 MDT.

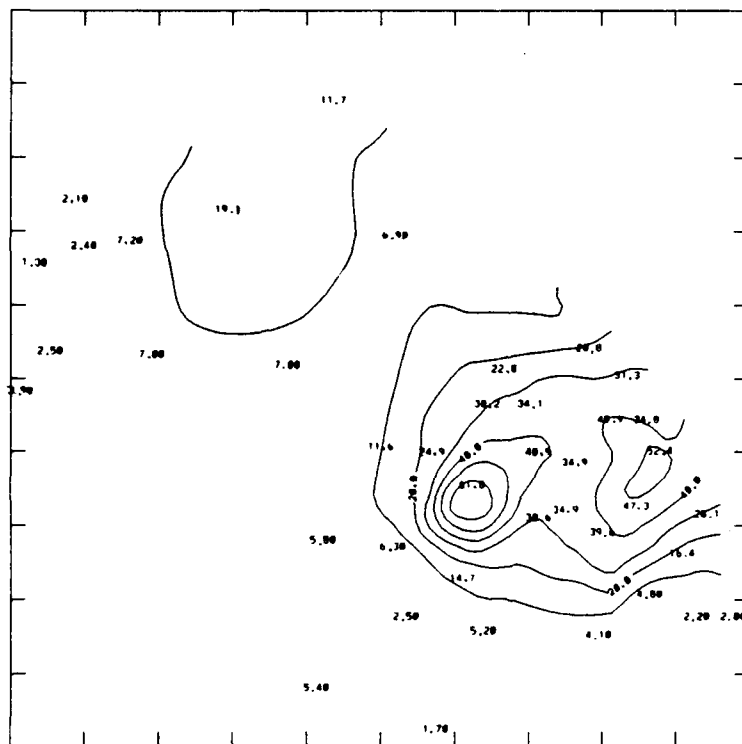


Figure 4.10. Radar rainfall estimated using  $Z = 200R^{1.6}$  and no threshold for 1550-1715 MDT.

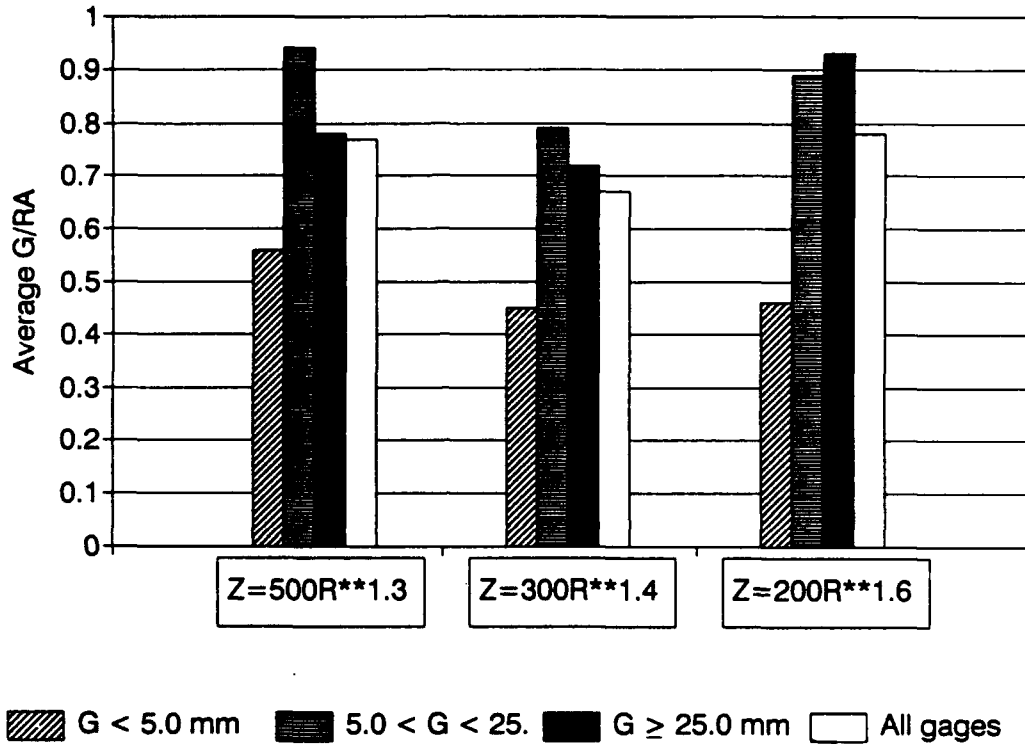


Figure 4.11. Average values of G/RA (gage rain/radar rain) for the entire storm (1550-1715 MDT) using three Z-R relations. Gage amounts are divided into four categories:  $\leq 5.0$  mm, 5-24.9 mm,  $\geq 25$  mm, and all amounts.

reduce errors in radar rainfall estimates. This is especially true in eastern Colorado where hail is a relatively common phenomena (Stout and Changnon, 1968). This section will introduce several hail detection methods currently in use and present radar evidence for the presence of hail during the June 6, 1991 storm.

### 1. Reflectivity thresholds

This is the simplest method suggested for using radar data to detect the presence of hail. Mason (1971) found 55 dBZ to be an effective threshold for the indication of hail. Researchers in Colorado (Kelsch, 1988 and 1989; Rasmussen et al., 1989) note that hail is generally observed on a typical thunderstorm day in this area once the reflectivity values reach the low 50's. During tests of the NEXRAD precipitation algorithms during the summer of 1988, Kelsch (1989) and Rasmussen et al. (1989) noted that Denver area meteorologists sharply criticized the NEXRAD precipitation measurements for their large overestimates. Accuracy improved and area meteorologists became more confident in the estimates after the reflectivity threshold was lowered from 60 dBZ to 50 dBZ. However, this method carries the risk of greatly underestimating the infrequent heavy rain events in which hail is not a factor.

Measurements of differential propagation constant ( $K_{DP}$ ) provide some support for the use of a threshold. A phase difference ( $\phi_{DP}$ ) between vertically and horizontally polarized signals develops as the radar beam propagates through an anisotropic precipitation medium like rain. The differential propagation constant is a measure of the rate of change of  $\phi_{DP}$  with range. The differential propagation constant has been found useful in discriminating between hail and rain in a mixture.

Balakrishnan and Zrnić (1990a) found that the curve for the  $Z-K_{DP}$  relation in rain (from measurements in Oklahoma) and the boundary separating pure rain from mixed precipitation became coincident at 55.6 dBZ. Caution must be used in applying this result to a Colorado thunderstorm.

The peak reflectivity values during the June 6 storm were generally 55 to 60 dBZ, suggesting that hail occurred. Numerous ground reports confirmed that hail indeed fell (see Chapter 2). The use of a threshold appears warranted in this case and does in fact result in an improvement in rainfall estimates. Figure 4.12a shows storm total rainfall with a 55 dBZ threshold, i.e. any  $Z$  value greater than 55 dBZ is set equal to 55 dBZ. The location of maximum rainfall changes only slightly, but a large reduction in magnitude is apparent. Figure 4.12b shows radar rainfall with a 50 dBZ threshold. The radar rainfall field is now quite close to the actual rainfall pattern, but the area of heaviest rainfall is now slightly underestimated.

Figure 4.13 shows  $G/RA$  for light, moderate, and heavy rain amounts with 50 dBZ, 55 dBZ, and no threshold. The average  $G/RA$  for all gages becomes closer to 1.0 with the use of a threshold. Estimates for gages receiving light rain ( $\leq 5$  mm) are not changed with a 55 dBZ threshold and changed only slightly by a 50 dBZ threshold. Estimates for gages receiving heavy rain ( $\geq 25.0$  mm) improve the most with the use of a threshold. For these gages the average  $G/RA$  is 0.76 with no threshold, 0.81 with a 55 dBZ threshold, and improves to 1.06 (small underestimate) with a 50 dBZ threshold. Large underestimates would obviously occur if the 50 dBZ threshold was used for a storm producing heavy rain and no hail.

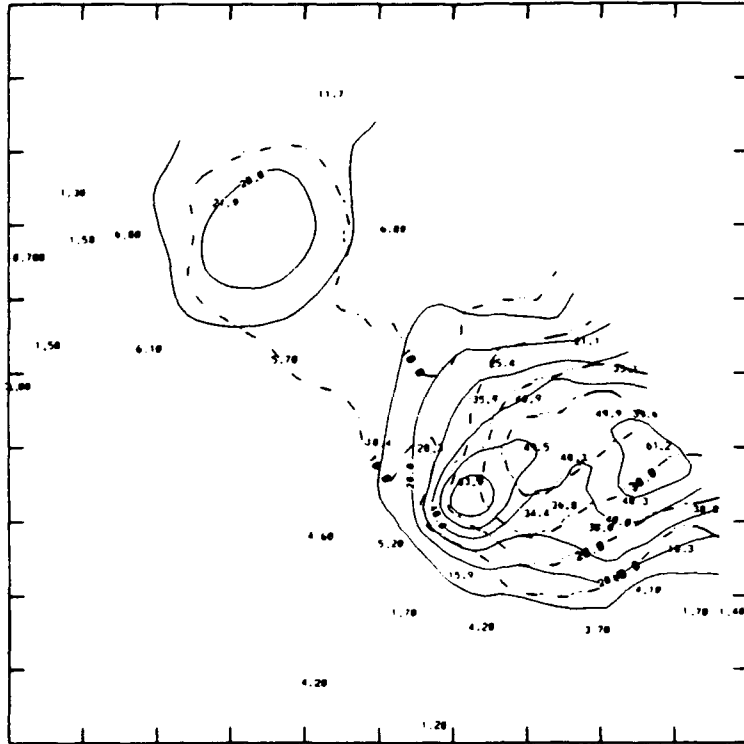


Figure 4.12a. Total radar rain (1550-1715 MDT) estimated with  $Z = 500R^{1.3}$  and a 55.0 dBZ threshold. Dashed lines indicate rain gage totals.

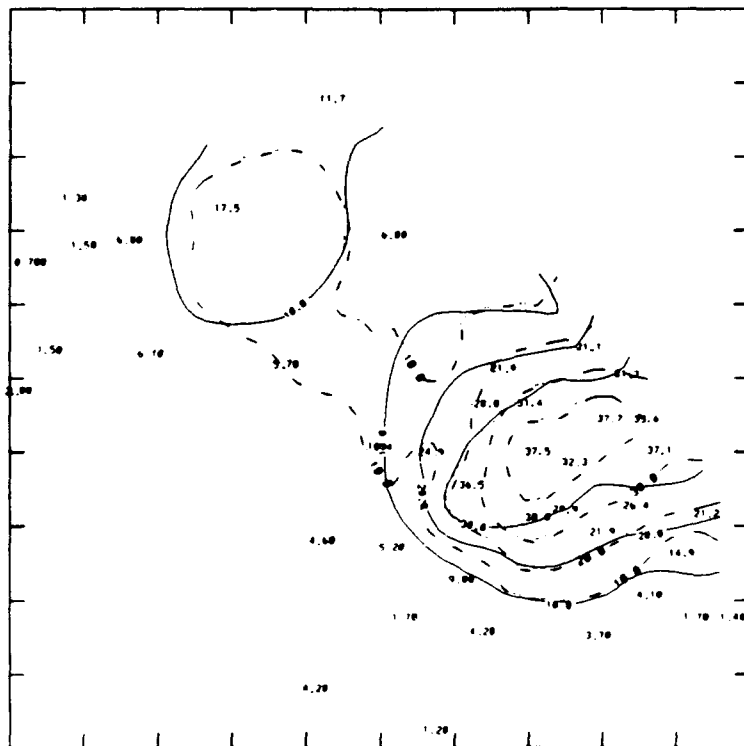


Figure 4.12b. Same as above, but with a 50.0 dBZ threshold.



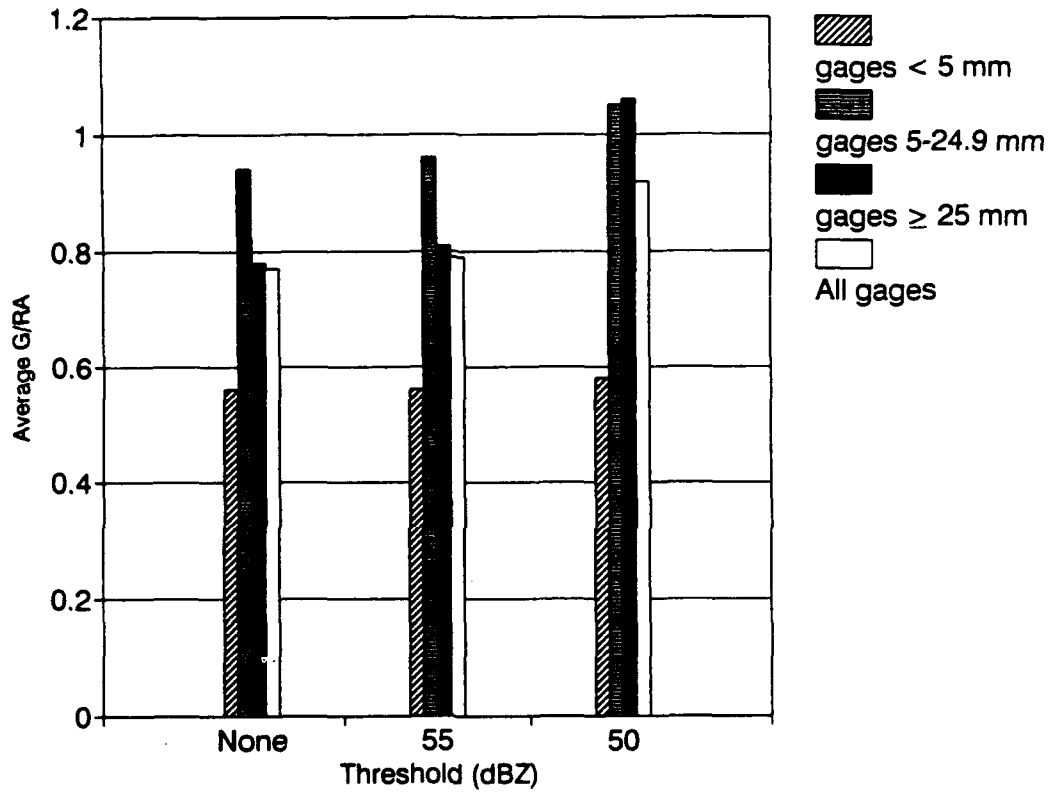


Figure 4.13. Average G/RA for the entire period (1550-1715 MDT) using threshold of 50 dBZ and 55 dBZ and no threshold. Z-R relation:  $Z = 500R^{1.3}$ .

## 2. Differential Reflectivity ( $Z_{DR}$ ) and Hail Detection Signal ( $H_{DR}$ )

Differential reflectivity is defined by Seliga and Bringi (1976) as

$$Z_{DR} = 10 \log \left( \frac{Z_{HH}}{Z_{VV}} \right) \quad (8)$$

where  $Z_{HH}$  and  $Z_{VV}$  are the copolar horizontal and vertical reflectivities, respectively. Observations have shown that raindrops are oblate spheroids which tend to fall with their short axis oriented vertically (McCormick et al., 1972). This feature causes rain to be characterized by values of  $Z_{DR} > 0$ . Bringi et al. (1986) found rain to have  $Z_{DR} > 0.5$  with  $Z$  variable, but generally less than 60 dBZ. Larger raindrops are more oblate and therefore produce larger  $Z_{DR}$  values.

In contrast, hail is generally more spherical with an average axis ratio near 0.8 (Knight, 1986) and often tumbles as it falls. Large hail tends to be less spherical and has been observed to fall with its long axis oriented vertically, giving negative  $Z_{DR}$  values (Aydin et al., 1986). Because of these properties,  $Z_{DR}$  measurements of hail are generally near zero or slightly negative. Mixtures of rain and hail can make the interpretation of  $Z_{DR}$  measurements more difficult, but since  $Z_{DR}$  is a measure of reflectivity weighted oblateness the hail portion of the mixture usually dominates (Jameson, 1983). Despite the fact that the hail portion of the mixture will dominate the  $Z_{DR}$  signal, raindrops will raise the  $Z_{DR}$  value to some degree. For Rayleigh scatterers the backscattering cross section increases with increasing thickness of the water coating; in addition  $Z_{DR}$  is enhanced (Aydin et al., 1984). In other words, hailstones with their minor axis oriented vertically will exhibit a more positive  $Z_{DR}$  (or more negative  $Z_{DR}$  with the minor axis oriented horizontally) as the hailstone melts

and becomes water coated. Since reflectivity is also enhanced by a water coating, the average  $Z_{DR}$  and  $Z$  values should increase below the  $0^{\circ}\text{C}$  level. Aydin et al. (1990) found this to be the case during the severe Denver hailstorm of 13 June 1984.

Aydin et al. (1986) introduced a hail detection signal  $H_{DR}$  based on measurements taken near Boulder, Colorado and in central Illinois. They obtained 2217 dropsize distributions (confirmed to be rain only by observers at the disdrometer site) and computed the corresponding values of  $Z$  and  $Z_{DR}$ . Figure 4.14 (from Aydin et al., 1986) shows a scatter plot of these values with a rather distinct upper bound on  $Z$  apparent. This boundary is approximated by Eq. (9), with  $(Z, Z_{DR})$  pairs outside of the boundary assumed to be hail or a rain/hail mixture.

$$f(Z_{DR}) = \begin{cases} 27, & Z_{DR} \leq 0 \text{ (dB)} \\ 19Z_{DR} + 27, & 0 \leq Z_{DR} \leq 1.74 \text{ (dB)} \\ 60, & Z_{DR} > 1.74 \text{ (dB)} \end{cases} \quad (9)$$

The hail detection signal is defined by:

$$H_{DR} = Z_H - f(Z_{DR}). \quad (10)$$

The higher the value of  $H_{DR}$  (i.e. the further the  $Z, Z_{DR}$  pair is from the rain boundary) the more likely it is that the sample contains hail.  $H_{DR}$  values calculated from measurements obtained below the  $0^{\circ}\text{C}$  level are considered to be the most reliable. Positive  $H_{DR}$  values above the  $0^{\circ}\text{C}$  level should still be indicative of hail, but could indicate other frozen hydrometeors as well (Aydin et al., 1990).

A simple algorithm was developed to compute  $H_{DR}$  for each scan in which  $Z_{DR}$  data is available. The values of  $Z$  and  $Z_{DR}$  at each pixel in the 3.5 km MSL

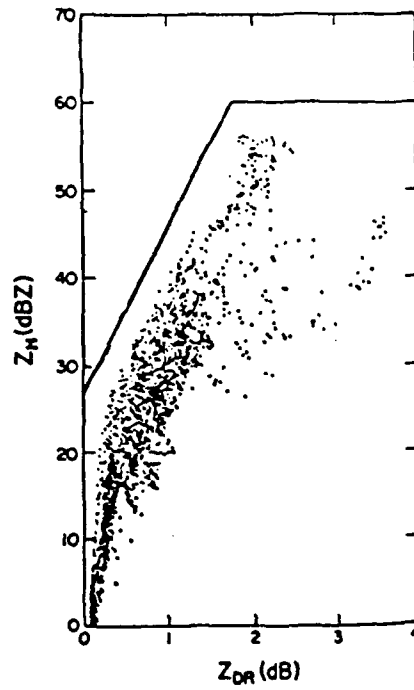


Figure 4.14. Scatter plot of  $Z$  (dBZ) versus  $Z_{DR}$  computed from 2217 dropsize distributions (from Aydin et al., 1986).

CAPPI ( $0^{\circ}\text{C}$  level is 3.8 km) are used to compute  $H_{\text{DR}}$ . Negative  $H_{\text{DR}}$  values are set to zero because they indicate hail is not present. The  $H_{\text{DR}}$  often provides a clearer picture than the frequently noisy  $Z_{\text{DR}}$  field. Near-zero  $Z_{\text{DR}}$  values sometimes occur with low  $Z$  values; these areas are unlikely to contain hail and the  $H_{\text{DR}}$  field shows this.

Since hail was confirmed by ground reports during the June 6 storm,  $Z_{\text{DR}}$  and  $H_{\text{DR}}$  fields should show evidence of this. Unfortunately  $Z_{\text{DR}}$  measurements were available for only six (V4, V9, V13, V23, V28, and V33) of the 18 sample volumes. Several usable volumes did reveal interesting results, however. The first  $Z_{\text{DR}}$  scan (V4) covered 1555-1600 MDT, during which time the strongest portion of the storm was over gages 720, 820, and 830. Figure 4.15a shows the reflectivity field at 3.5 km, with only  $Z > 30$  dBZ plotted. The  $Z_{\text{DR}}$  field at 3.5 km MSL is plotted in Figure 4.15b, with  $Z \geq 50$  dBZ plotted as well. A large area of  $Z_{\text{DR}}$  less than or near zero is colocated with the region of high ( $> 50$  dBZ) reflectivity values, providing a strong indicator of hail.

The northwestern quadrant of this scan seems to be effected by some type of interference; note the alternating pattern of  $Z_{\text{DR}} > 0.5$  dB and  $Z_{\text{DR}} < 0.5$  dB. A spiral-type pattern was evident in both the  $Z$  and  $Z_{\text{DR}}$  fields when the entire scan was examined. This type of pattern is indicative of interference from another radar of similar wavelength (Pat Kennedy of the CSU-CHILL radar, personal communication). Normalized Correlated Power (NCP) values are low in this region, providing further indication that a problem exists. Scans V9 and V13 display the same type of interference.  $Z_{\text{DR}}$  values in regions where  $Z < 20$  dB will be considered unreliable and not used.

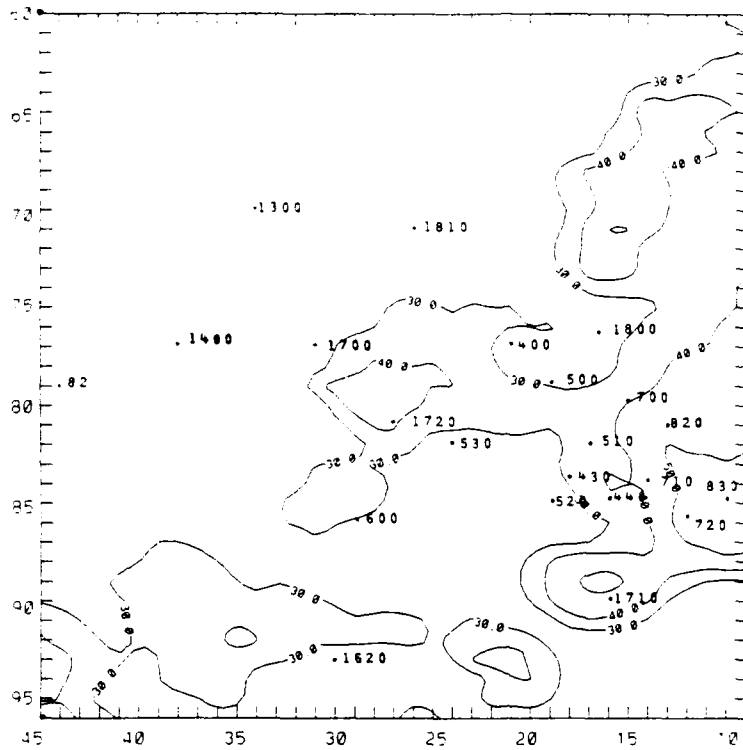


Figure 4.15a.

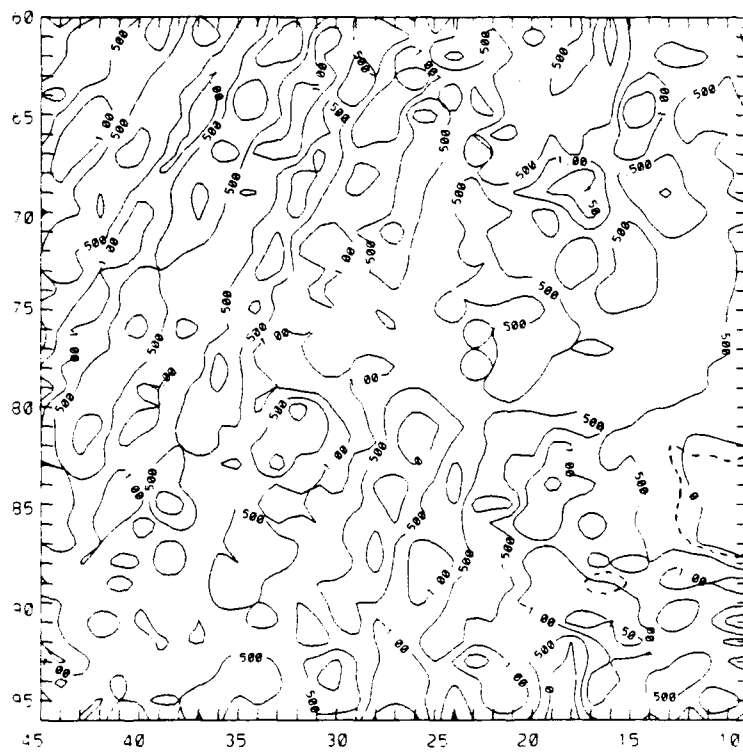


Figure 4.15b.

Figure 4.15. V4 (1555-1600 MDT) a) reflectivity (dBZ) and b)  $Z_{DR}$  (dB) at 3.5 km MSL. Dashed lines in b) indicate areas of reflectivity 50 dBZ or above.

The hail detection signal reached a maximum value of 30 dB at gage 830, with values of 22.2 and 17.3 dB at gages 720 and 820, respectively (see Figure 4.15c). The radar overestimated rainfall by an average of 7.7 mm (0.30 in) at these gages during this 5 minute period. In general, regions of positive  $H_{DR}$  were colocated with  $Z$  values greater than 45 dBZ. Hail was in fact reported near gage 830 in a special weather statement issued by the NWS at 1605 MDT.

During scan V9 (1605-1610 MDT) the thunderstorm cell was located approximately 5 km west of its previous position. Gages 440, 710, and 820 were in a region with  $Z > 50$  dBZ (Figure 4.16a), with  $Z_{DR}$  values near zero for these gages (Figure 4.16b). As in the previous scan, the region of reflectivity values above 50 dBZ coincided fairly well with the low  $Z_{DR}$  region. However, the western edge of the thunderstorm exhibited values of  $Z_{DR}$  approaching 1.0 dB. A plot of  $H_{DR}$  for this scan (Figure 4.16c) also suggests the presence of hail. Gages 440, 710, and 820 had  $H_{DR}$  values of 26.2, 30.0, and 27.0 dB, respectively. Radar overestimates for these gages averaged 12.3 mm (0.48 in) in only 5 minutes. Hail 1.0 inch in diameter was reported in Aurora at 1609 MDT, confirming the presence of hail in this thunderstorm cell.

Hail contamination during V4 and V9 appears to be the likely cause of the previously discussed false radar rain maxima in the vicinity of gages 440, 710, and 820. Figure 4.17a is a scatter plot of  $Z_{DR}$  versus the error in radar estimates ( $RA - G$ ). The largest errors are associated with low ( $< 0.5$  dB)  $Z_{DR}$  values, which are indicative of hail. The higher  $Z_{DR}$  values associated with rain generally result in small overestimates, possibly due to evaporation. A similar plot of  $H_{DR}$  (Figure 4.17b)

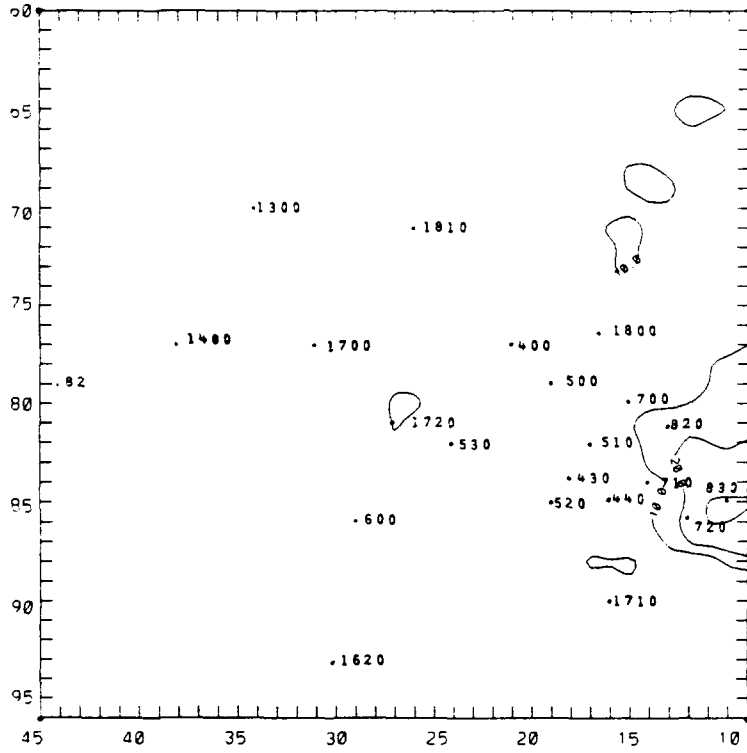


Figure 4.15c.

Figure 4.15. V4 (1555-1600 MDT) c)  $H_{DR}$  (dB) at 3.5 km MSL.



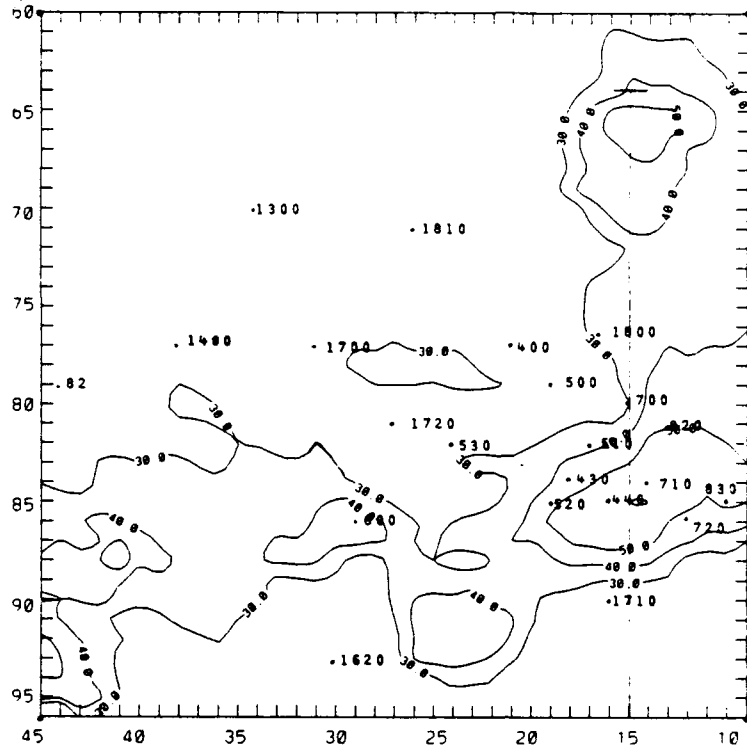


Figure 4.16a.

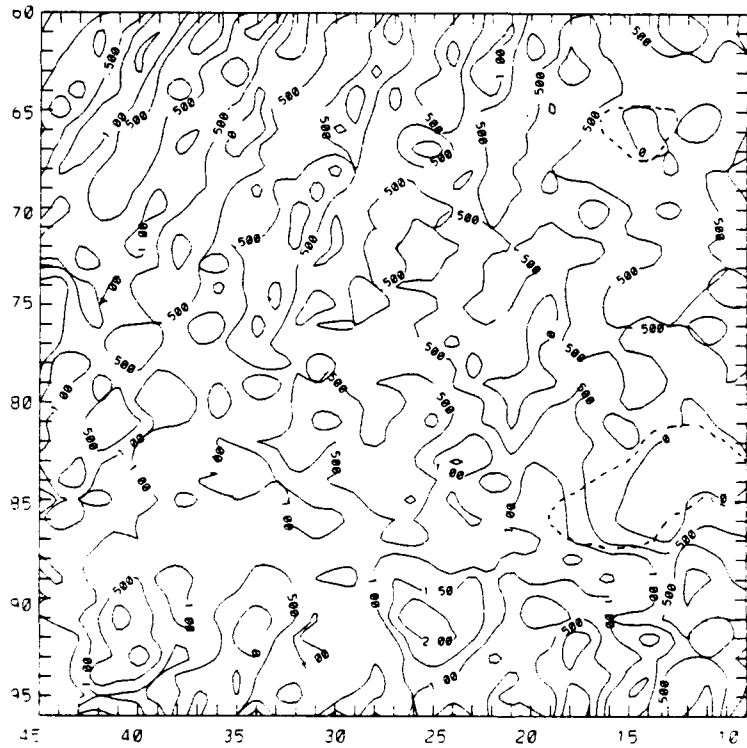


Figure 4.16b.

Figure 4.16. V4 (1605-1610 MDT) a) reflectivity (dBZ) and b)  $Z_{DR}$  (dB) at 3.5 km MSL. Solid line in a) indicates the cross section shown in Fig. 4.18. Dashed lines in b) indicate areas of reflectivity 50 dBZ or above.

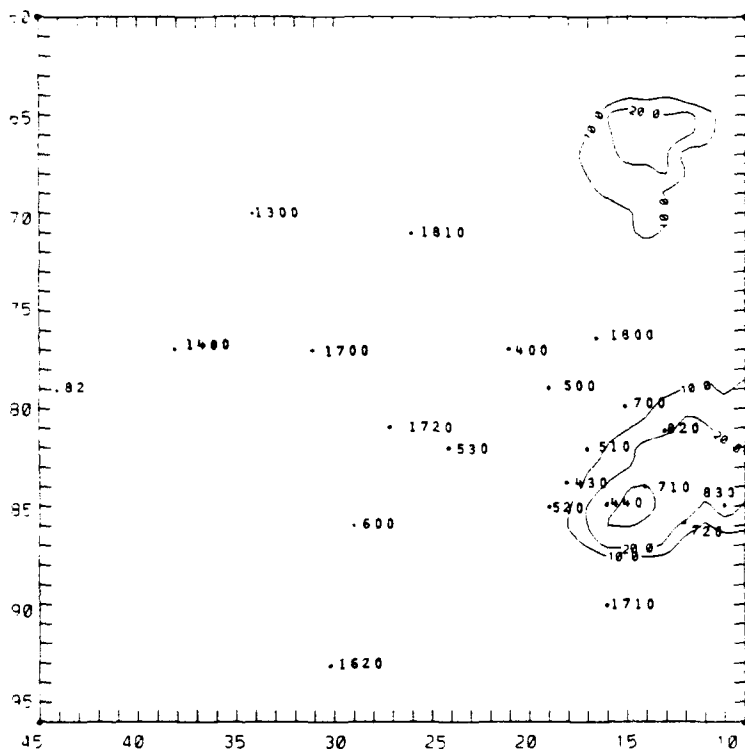


Figure 4.16c.

Figure 4.16. V9 (1605-1610 MDT) c)  $H_{DR}$  (dB) at 3.5 km MSL.

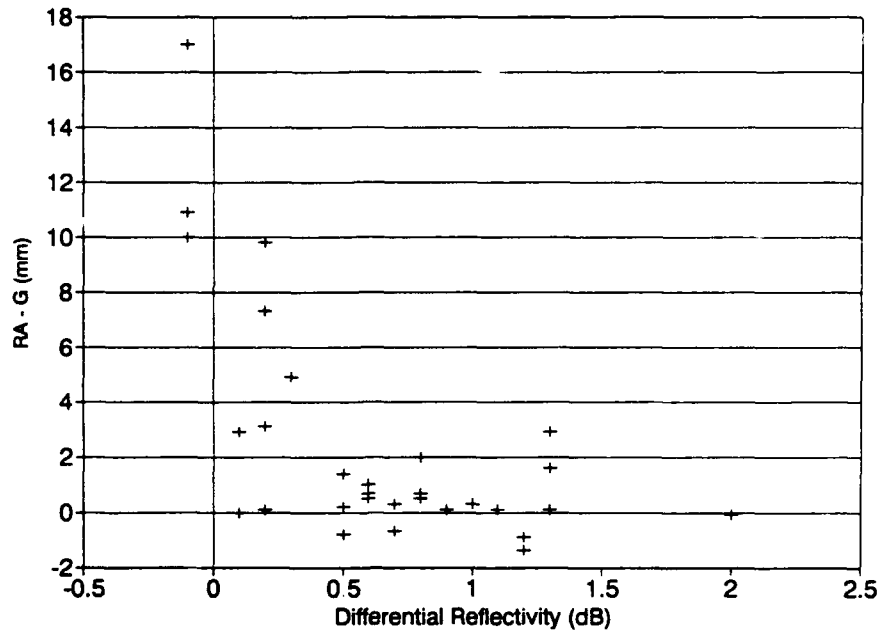


Figure 4.17a. Scatter plot of  $Z_{DR}$  versus (RA - G) for scans V4 and V9 at 3.5 km MSL.

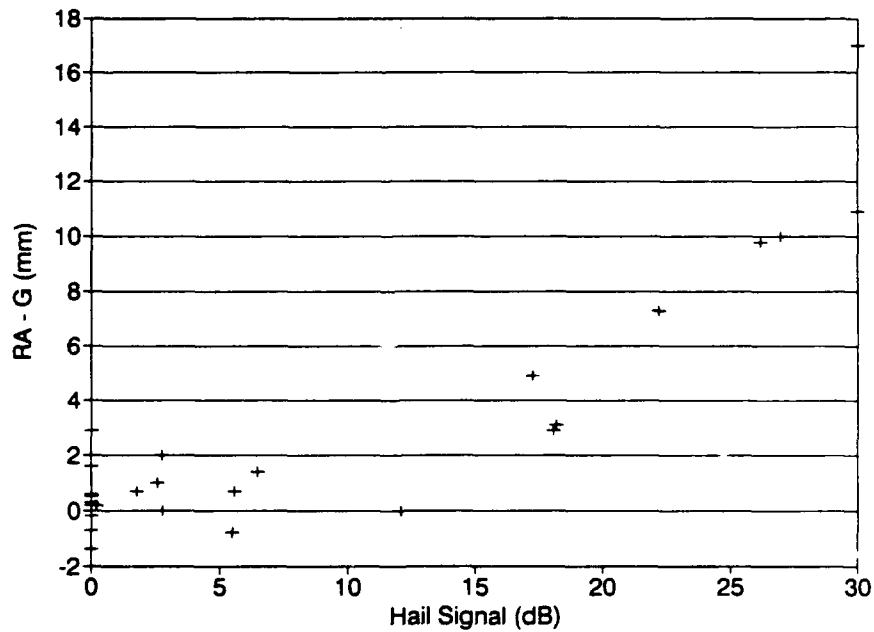


Figure 4.17b. Scatter plot of  $H_{DR}$  versus (RA - G) for scans V4 and V9 at 3.5 km MSL.

shows the largest errors to be associated with positive  $H_{DR}$  values, another indication of hail.

Figure 4.18a is a north-to-south cross section of the thunderstorm during scan V9 at 3.5 km MSL. The cross section passes through the core of the storm at  $X = 15$  (see Figure 4.16a).  $Z_{DR}$  drops toward zero in the high-reflectivity cores of the two thunderstorm cells, but rises to levels associated with rain in the less intense regions. A cross section of  $H_{DR}$  through the same area (Figure 4.18b) shows strong peaks in the cells where  $Z$  and  $Z_{DR}$  suggest hail is present.

Figure 4.19a presents a vertical profile of  $Z$  and  $Z_{DR}$  above gage 710, while Figure 4.19b shows the same profiles above gage 430. Both profiles are from scan V9. These values are derived by averaging the pixel nearest the gage and the surrounding eight pixels. Above gage 710 the reflectivity remained greater than 50 dBZ up to the 7.4 km AGL level, and then dropped sharply above that level. Differential reflectivity remained slightly negative through the entire depth of the  $\geq 50$  dBZ region, and changed very little near the  $0^{\circ}\text{C}$  level (2.2 km AGL). This pattern suggests that hail dominated the  $Z_{DR}$  signal, even below the  $0^{\circ}\text{C}$  level where the presence of droplets might be expected to raise  $Z_{DR}$  values. It appears that little or no rain was present with the hail here, since gage 710 recorded no precipitation, while the radar estimated 17.0 mm (0.67 in). Gage 430, located 3.5 km west of 710, has a more complex vertical profile of  $Z$  and  $Z_{DR}$ . Reflectivity values remained near 45 dBZ below the  $0^{\circ}\text{C}$  level, but increased sharply above this level. This profile is probably due to the westward tilt of the thunderstorm cell with height. Differential reflectivity values decreased steadily from 1.0 dB at 3.1 km to 0.1 dB at 3.9 km AGL. Melting of ice particles probably caused the increasing  $Z_{DR}$  values in the lower levels.

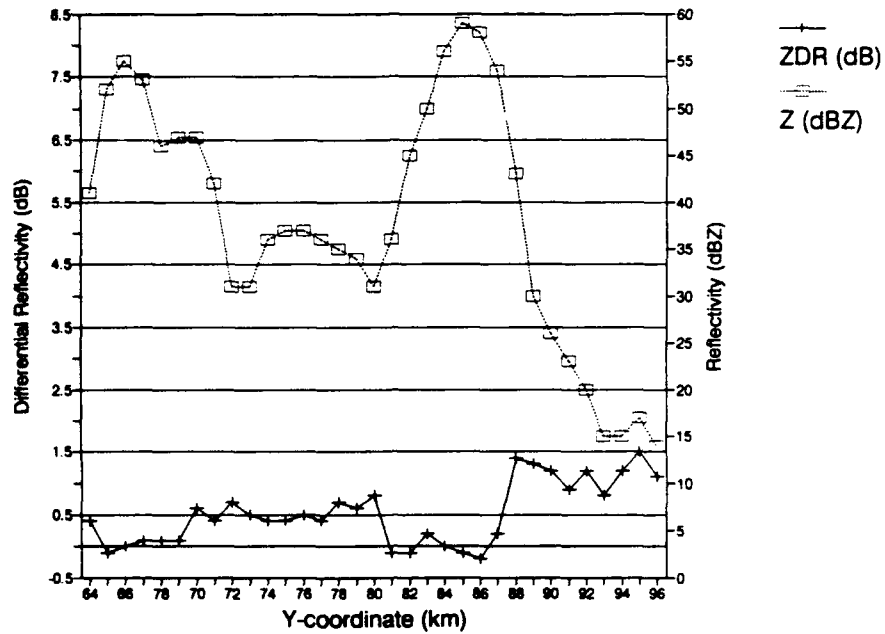


Figure 4.18a. North-to-south cross section of the thunderstorm during V9 (1605-1610 MDT) at 3.5 km MSL. The cross section passes through  $X = 15$  km (see Fig. 4.16).

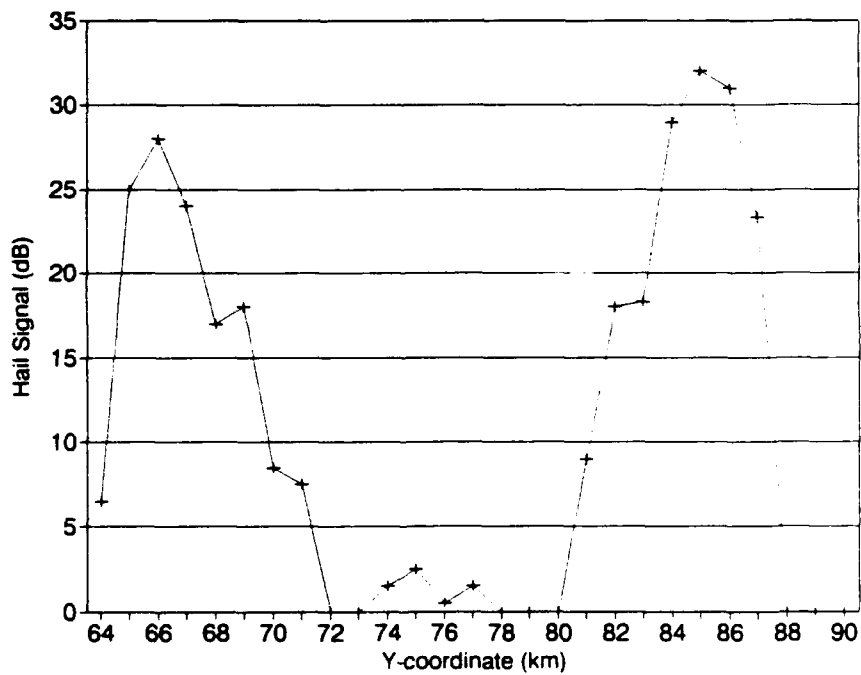


Figure 4.18b. Same cross section as Fig. 4.18a, but showing  $H_{DR}$ .

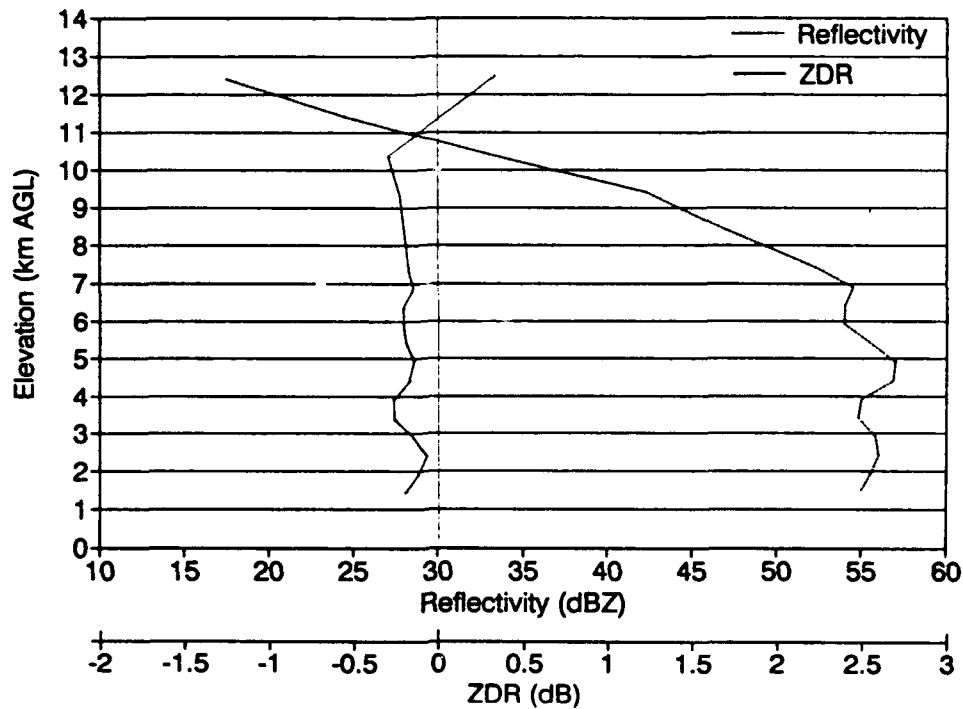


Figure 4.19a. Vertical profiles of Z (dBZ) and  $Z_{DR}$  (dB) above gage 710.

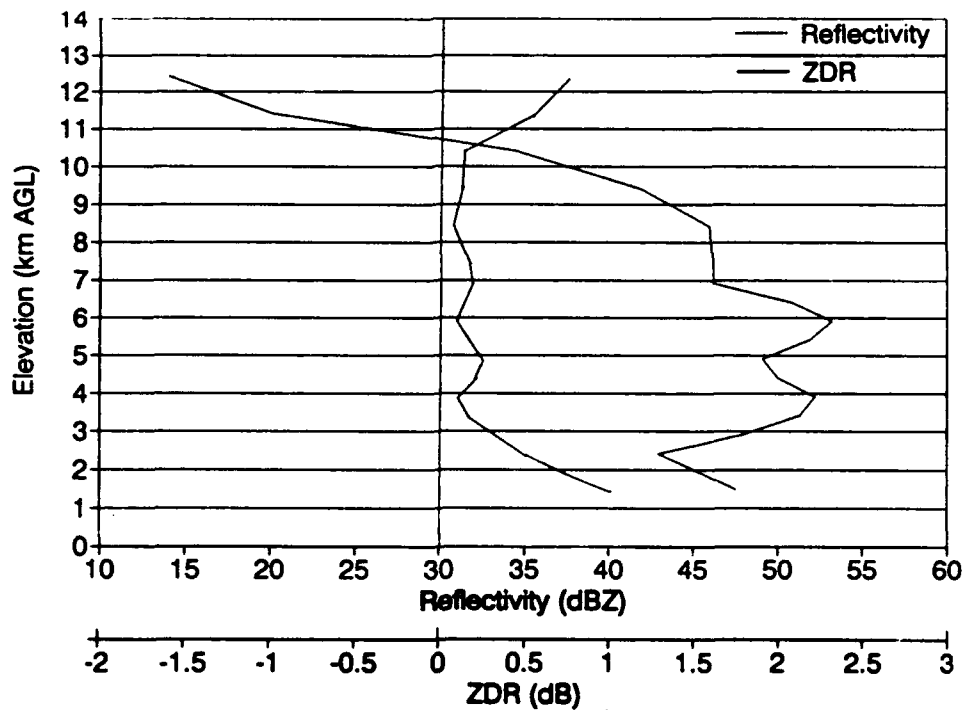


Figure 4.19b. Same as above, but above gage 430.

The peaks in the Z profile at 3.9 km and 5.9 km AGL correspond to minima in the  $Z_{DR}$  profile, suggesting that higher concentrations of hail may have enhanced reflectivity at those levels. While hail appeared to be present aloft, it was absent at the 1.9 km AGL level which was used to make the radar rainfall estimates and  $H_{DR}$  calculations. Gage 430 recorded 1.0 mm, while the radar estimated 1.7 mm.

Scan V13 (1615-1620 MDT) unfortunately missed the eastern portion of the storm during the 0.8 degree sweep. For this reason, data from the 4.3 km MSL level was used to capture the missing section of the storm. Reflectivity tended to be higher, while  $Z_{DR}$  values were slightly lower at this increased elevation. Gages 440, 700, 710, 810, and 820 were all below regions of  $\geq 50$  dBZ reflectivity (Figure 4.20a), with the associated  $Z_{DR}$  values less than 0.2 dB (Figure 4.20b). The radar overestimated rainfall at each of these gages. The average overestimate was 3.9 mm, with a maximum of 12.9 mm at gage 710. Three gages (430, 510, and 520) had Z values less than 50 dBZ at 3.5 km MSL, but at 4.3 km MSL all had Z greater than 50 dBZ. This results in rainfall underestimates using 3.5 km data, but overestimates using data at 4.3 km. This illustrates the danger of using data from different heights, especially if any direct comparisons are to be made.

### 3. Difference Reflectivity ( $Z_{DP}$ )

The difference reflectivity ( $Z_{DP}$ ) is another polarimetric measurement which has been used to gain information about the presence of hail or other solid hydrometeors within thunderstorms (Meischner et al., 1991; and Golestani et al., 1989). The difference reflectivity is defined as

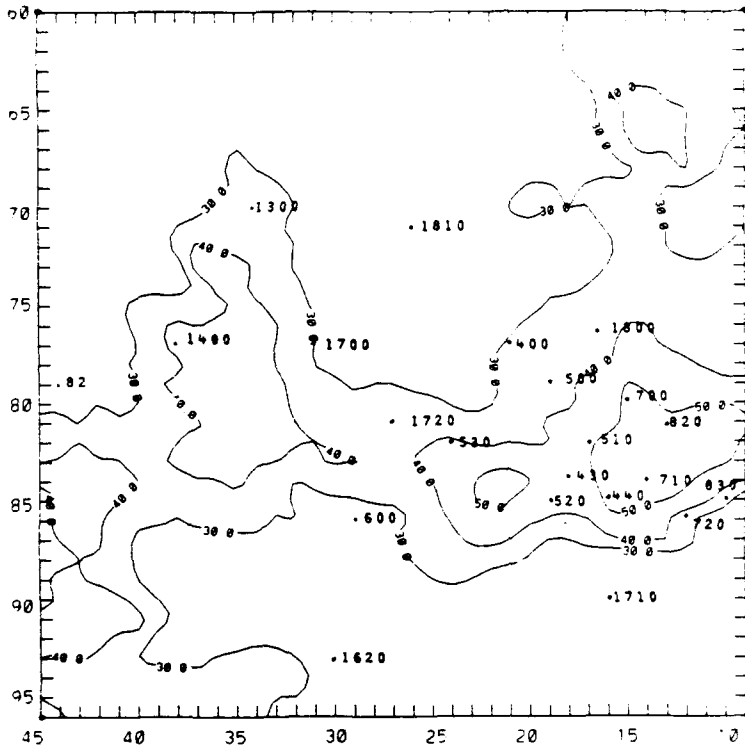


Figure 4.20a.

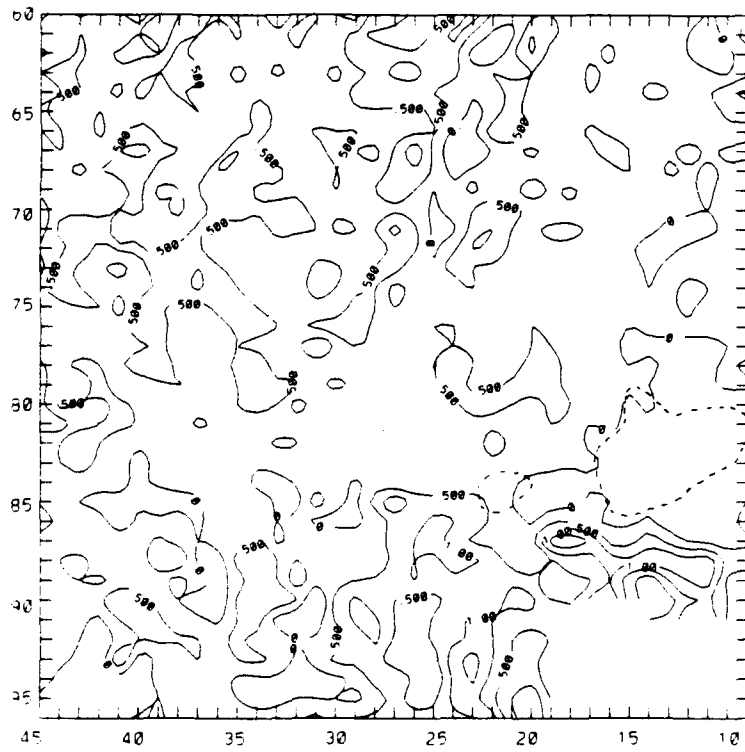


Figure 4.20b.

Figure 4.20. V13 (1615-1620 MDT) a) reflectivity (dBZ) and b)  $Z_{DR}$  (dB) at 4.3 km MSL. Dashed lines in b) indicate areas of reflectivity 50 dBZ or above.



$$Z_{DP} = 10 \log(Z_H - Z_V). \quad (11)$$

Hail, which is nearly spherical or tumbling ( $Z_H = Z_V$ ), will give only a small contribution to  $Z_{DP}$ , but it will contribute to total  $Z$ . In a mixture of rain and hail, only the rain portion of the mixture will contribute to  $Z_{DP}$  due to the much more oblate shape of raindrops. Golestani et al. (1989) plotted  $Z_{DP}$  versus  $Z_H$  for several gamma raindrop size distributions and used the linear relation they found between the two to define a "rain line". A scatter plot of the same type for rain regions during V4 (Figure 4.21) yields a very similar rain line, with a correlation coefficient of 0.975. This plot is composed of 168  $Z_H$ ,  $Z_{DP}$  pairs at 2.8 km MSL, or 1 km below the 0°C level. Large deviations from this line are usually the result of the presence of ice with the rain. The ice raises the reflectivity, but has little effect on  $Z_{DP}$ , therefore the  $Z$ ,  $Z_{DP}$  pair will not fall near the rain line.

Figure 4.22a is a scatter plot of 25  $Z$ ,  $Z_{DP}$  pairs at 3.2 km MSL during V4. These points are from a 5 km by 5 km area in the northeastern quadrant of the study area ( $X = 14$  to  $18$  km west and  $Y = 68$  to  $72$  km south of the radar). The arrangement of the values is still very linear, with a correlation coefficient of 0.867, and the points lie very close to the rain line. This indicates rain was still the primary component of the mixture at this level.

Golestani et al. (1989) introduced a method of quantifying the relative contributions of the rain and ice components of the mixture to the total reflectivity. The value of  $Z_H$  (rain) which corresponds to the  $Z_{DP}$  measured at a certain level can be inferred from the rain line in Figure 4.21. In other words,  $Z_{DP}$  provides a way to calculate the contribution of rain alone to the total reflectivity. Therefore the

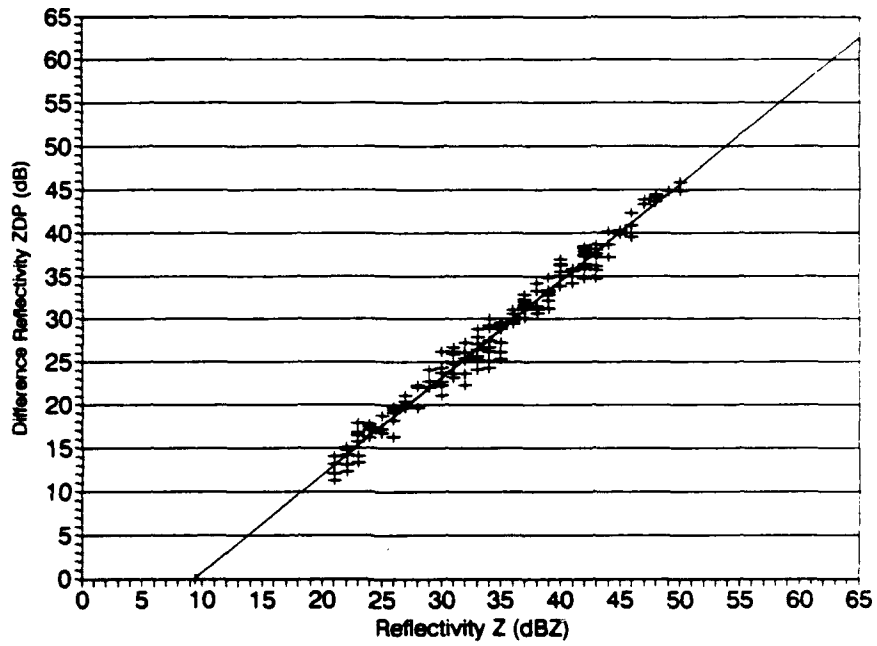


Figure 4.21. Scatter plot of  $Z_{DP}$  versus  $Z_H$  for V4 at 2.8 km MSL. The plot is composed of 168  $Z_H$ ,  $Z_{DP}$  pairs with  $Z_{DR}$  values above 0.4 db. The least squares fit line is described by  $Z_{DP} = 1.125 Z_H - 10.56$ , with  $R^2 = 0.975$ .

reflectivity-weighted fraction of rain  $f_r$  can be written as

$$f_r = \frac{Z_H(\text{rain})}{Z_H(\text{rain}) + Z_H(\text{ice})} \quad (12)$$

where the numerator is found using the rain line and the denominator is the total reflectivity measured by the radar.

The deviation from the rain line is found by assuming a reference value of  $Z$ , 45 dBZ for example. A scatter plot of  $Z$  versus  $Z_{DP}$  is made for the level of interest and a least squares linear fit to the data is performed (see Figures 4.22a and b). From this new line the value of  $Z_{DP}$  corresponding to  $Z_H = 45$  dBZ is found. The rain line is then used to find the  $Z_H = Z_H(\text{rain})$  value for  $Z_{DP}$ , since  $Z_{DP}$  measures the contribution of rain to  $Z_H$  at the level in question. The deviation from the rain line is  $45 \text{ dBZ} - Z_H(\text{rain})$ ; at 3.2 km MSL this value was 1.2 dB, showing rain was still the primary component of the mixture at this level. This deviation should increase, while  $f_r$  should decrease as the  $0^\circ\text{C}$  level is approached and exceeded. A plot of  $Z$ ,  $Z_{DP}$  at 3.5 km (Figure 4.22b) shows the linear nature of the data to be less apparent (correlation coefficient = 0.37), with the points falling farther from the rain line as well. The deviation from the rain line in this case was 4.9 dB.

Plots of rain fraction and deviation from the rain line with height (Figures 4.22c and d) illustrate the rapid change in the lowest 1 km from primarily rain to an ice-dominated mixture. The  $0^\circ\text{C}$  level on this date was approximately 2.2 km AGL. Radar samples from the 3.5 km level, which are used in this study, clearly will experience the effects of ice contamination. Unfortunately, this is the lowest level

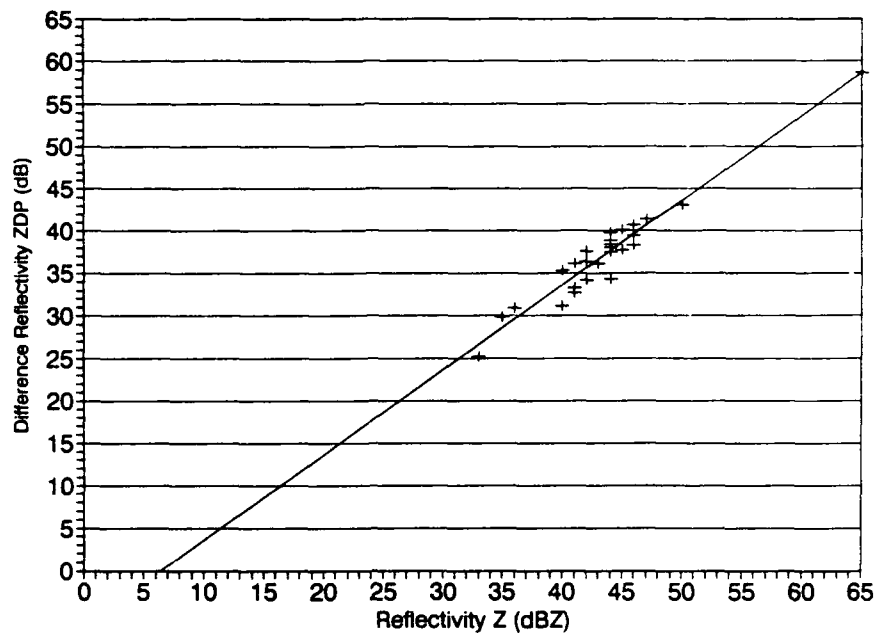


Figure 4.22a. Scatter plot of  $Z_{DP}$  versus  $Z_H$  for V4 at 3.2 km MSL.  
 $Z_{DP} = 1.002 Z_H - 6.4$ ,  $R^2 = 0.867$ .

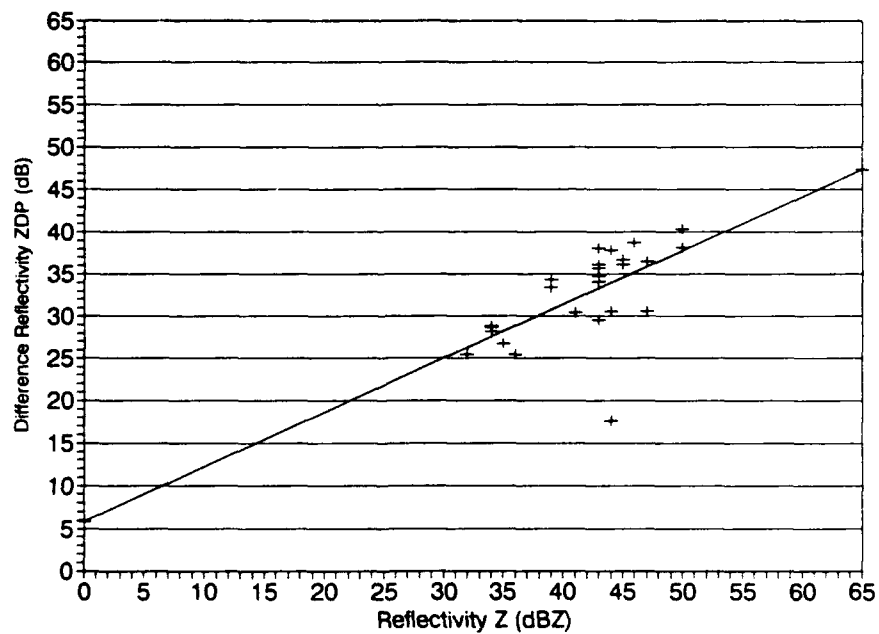


Figure 4.22b. Scatter plot of  $Z_{DP}$  versus  $Z_H$  for V4 at 3.5 km MSL.  
 $Z_{DP} = 0.64 Z_H + 5.84$ ,  $R^2 = 0.366$ .

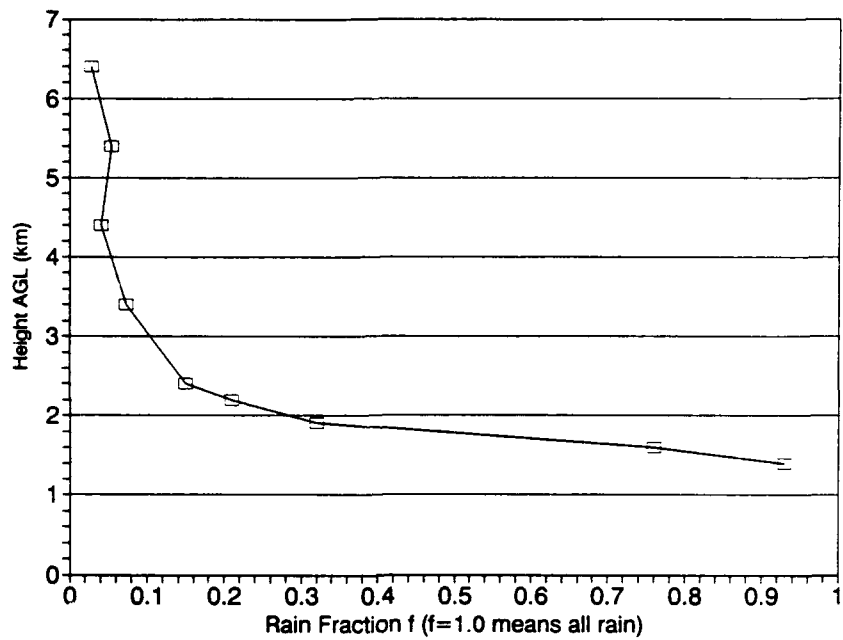


Figure 4.22c. V4 rain fraction,  $f$  as a function of height (km AGL).  
 $0^{\circ}\text{C}$  level is 2.2 km AGL.

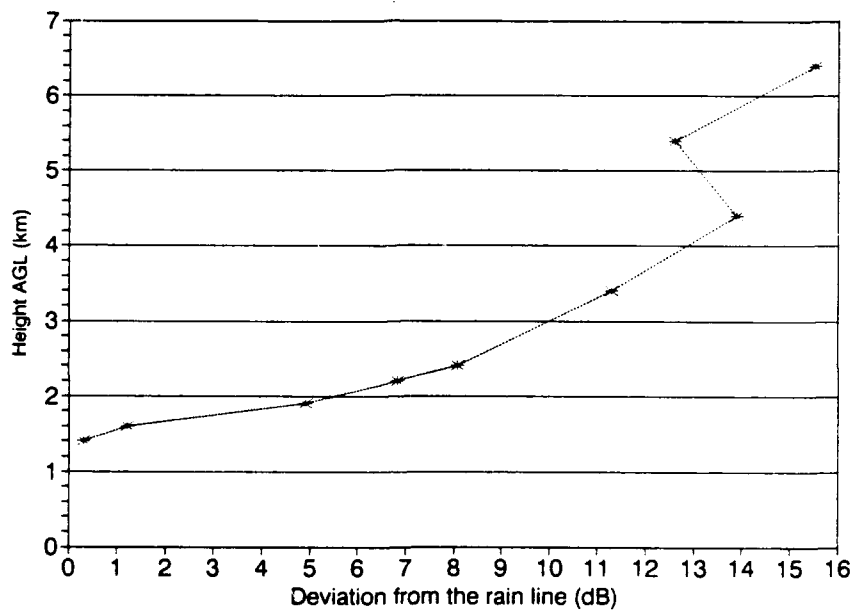


Figure 4.22d. V4 deviation from the rain line as a function of height (km AGL).  
 $0^{\circ}\text{C}$  level is 2.2 km AGL.

Author: David Joseph Speltz

Thesis Title: A Comparison of Radar Rainfall Estimates and Rain gage  
Measurements During Two Denver Thunderstorms

Rank/Branch: Captain/USAF

Date: 1992

Pages: 83

Degree: MS in Meteorology

Institution: Colorado State University

## ABSTRACT

### A COMPARISON OF RADAR RAINFALL ESTIMATES AND RAIN GAGE MEASUREMENTS DURING TWO DENVER THUNDERSTORMS

During the summer of 1991 Colorado State University's (CSU) Department of Atmospheric Science participated in an experiment which examined the usefulness of radar measurements in estimating thunderstorm rainfall. An array of 41 rain gages in Denver provided precipitation measurements to compare with the radar results. The first storm studied occurred on June 6 and produced up to 43.7 mm of rain in 85 minutes, while the August 5 storm produced a peak rain amount of 37.8 mm in 60 minutes.

Estimates of rainfall made by using a relation between the radar reflectivity ( $Z$ ) and the rain rate ( $R$ ) frequently display large errors. For example, overestimates as high as 58.5 mm occurred during the June 6 storm. During this storm the largest overestimates were associated with unusually high reflectivity values caused by hail. Hail was inferred from  $Z$ ,  $Z_{DR}$ ,  $H_{DR}$ , and  $Z_{DP}$  fields. Using a reflectivity threshold of 50 dBZ to account for hail contamination improved the average radar rainfall error from 8.0 mm to 3.5 mm. Although a threshold improved results during the June 6 event, this would not be the case for a storm with 50+ dBZ values and no hail. A 50 dBZ cap during the August 5 event only increased the errors. This study shows that radar rainfall estimates using Z-R relations provide good supplemental information, but will not replace traditional rain gages.

## CHAPTER VII

### REFERENCES

- Ahnert, P., M. Hudlow, E. Johnson, D. Green, and M. Dias, 1983: Proposed "on-site" precipitation processing system for NEXRAD. *Preprints, 21st Radar Meteorology Conference, Amer. Meteor. Soc.*, 378-385.
- Albers, S., K. Heideman, R. Jesuroga, M. Kelsch, J. Smart, J. Snook, E. Szoke, D. Walker, and H. Winston, 1988: PROFS final report to NEXRAD/JSPO for the 1988 fiscal year. NOAA/ERL/FSL/PROFS, Boulder, CO, 27-44.
- Atlas, D., and A.C. Chmela, 1957: Physical-synoptic variations of raindrop size parameters. *Preprints, Sixth Weather Radar Conference, Cambridge, MA. Amer. Meteor. Soc.*, 21-29.
- Atlas, D., and C.W. Ulbrich, 1990: Early foundations of the measurement of rainfall by radar. Chapter 12 in *Radar in Meteorology*, D. Atlas, Ed.), Amer. Meteor. Soc., Boston, MA.
- Aydin, K., and T.A. Seliga, 1984: Radar polarimetric backscattering properties of conical graupel. *J. Atmos. Sci.*, **41**, 1887-1892.
- \_\_\_\_\_, K., \_\_\_\_\_, and V. Balaji, 1986: Remote sensing of hail with dual linear polarization radar. *J. Climate Appl. Meteor.*, **25**, 1475-1484.
- \_\_\_\_\_, K., Y. Zhao, and T.A. Seliga, 1990: A differential reflectivity radar hail measurement technique: Observations during the Denver hailstorm of 13 June 1984. *J. Atmos. Oceanic Tech.*, **7**, 104-113.
- Balakrishnan, N. and D.S. Zrnic, 1990a: Estimation of rain and hail rates in mixed-phase precipitation. *J. Atmos. Sci.*, **47**, 565-583.
- \_\_\_\_\_ and \_\_\_\_\_, 1990b: Use of polarization to characterize precipitation and discriminate large hail. *J. Atmos. Sci.*, **47**, 1525-1540.
- Battan, L.J., 1973: **Radar Observation and the Atmosphere**. University of Chicago Press, Chicago IL.



- Brandes, E.A., and J.W. Wilson, 1986: Measuring storm rainfall by radar and rain gage. In **Thunderstorms: A Social, Scientific, and Technological Documentary**. Vol. 3: Instruments and Techniques for Thunderstorm Observation and Analysis (E. Kessler, Ed.), Second ed., University of Oklahoma Press, Norman, OK.
- Bringi, V.N., R.M. Rasmussen and J. Vivekanandan, 1986: Multiparameter radar measurements of Colorado convective storms, Part I: Graupel melting studies. *J. Atmos. Sci.*, **43**, 2345-2563.
- Burgess, D., and P.S. Ray, 1986: Principles of Radar. In *Mesoscale Meteorology and Forecasting* (P.S. Ray, Ed.), American Meteorological Society, Boston, MA.
- Dahlstrom, B., 1973. Investigation of errors in rainfall observations: a continued study. Report 34, Department of Meteorology, University of Uppsala, Sweden.
- Doviak, R., and D. Zrnić, 1984: **Doppler Radar and Weather Observations**. Academic Press, Orlando, FL, 480 pp.
- Doviak, R., D. Sirmans, and D. Zrnić, 1986: Weather radar. In **Thunderstorms: A Social, Scientific, and Technological Documentary**. Vol. 3: Instruments and Techniques for Thunderstorm Observations and Analysis (E. Kessler, Ed.), Second ed., University of Oklahoma Press, Norman, OK.
- Golestani, Y., V. Chandrasekar and V.N. Bringi, 1989: Intercomparison of multiparameter radar measurements. *Proc. 24th AMS Conference on Radar Meteorology, Amer. Meteor. Soc.*, 309-314.
- Jameson, A.R., 1983: Microphysical interpretation of polarization measurements in rain, Part I: Interpretation of polarization measurements and estimation of raindrop shapes. *J. Atmos. Sci.*, **40**, 1792-1802.
- Jones, D.M.A., 1966: The correlation of raingage-network and radar-detected rainfall. *Preprints, Twelfth Conference on Radar Meteorology*, Norman, OK. Amer. Meteor. Soc., 204-207.
- Joss, J., and A. Waldvogel, 1990: Precipitation measurement and hydrology. Chapter 29a in *Radar in Meteorology* (D. Atlas, Ed.), Amer. Meteor. Soc., Boston, MA.
- Kelsch, M., 1988: A meteorological assessment of the NEXRAD hydrology sequence for thunderstorms producing heavy rain. *Preprints, 15th Conference on Severe Local Storms*, Amer. Meteor. Soc., 209-212.

- \_\_\_\_\_, 1989: An evaluation of the NEXRAD hydrology sequence for different types of convective storms in northeastern Colorado. *Preprints, 24th Conference on Radar Meteorology*, Amer. Meteor. Soc., 207-210.
- Knight, N.C., 1986: Hailstone shape factor and its relation to radar interpretation of hail. *J. Climate Appl. Meteor.*, **25**, 1956-1958
- Larson, L.W., and E.L. Peck, 1974: Accuracy of precipitation measurements and hydrologic modeling. *Water Resour. Res.*, **10**, 857-863.
- Lipschutz, R.C., J.F. Pratte, and J.R. Smart, 1989: An operational  $Z_{DR}$ -based precipitation type/intensity product. *Preprints, 24th Conference on Radar Meteorology*, Amer. Meteor. Soc., 91-94.
- Mason, B.J., 1971: **The Physics of Clouds**. Clarendon Press, 672 pp.
- Marshall, J.S., and W.M. Palmer, 1948: The distribution of raindrops with size. *J. Meteor.*, **5**, 165-166.
- McCormick G.C., and B.L. Barge, 1972: The anisotropy of precipitation media. *Nature*, **238**, 214-216.
- Meischner, P.F., V. Bringi, D. Heimann, and H. Holler, 1991: A squall line in southern Germany: Kinematics and precipitation formation as deduced by advanced polarimetric and Doppler radar measurements. *Mon. Wea. Rev.*, **119**, 678-701.
- Mohr, C.G., L.J. Miller, and R.L. Vaughan, 1981: An interactive software package for the rectification of radar data to three-dimensional Cartesian coordinates. *Preprints, 21st Conference on Radar Meteorology*, Amer. Meteor. Soc., 569-574.
- NEXRAD, 1982: NEXRAD technical requirements (NTR). NEXRAD Joint System Program Office, Silver Spring, MD.
- NOAA, 1991: Preliminary Storm Data report, June 1991. WSFO Denver, CO.
- Rasmussen, E.N., J. Smith, J. Pratte, and R. Lipschutz, 1989: Real time precipitation accumulation estimation using the NCAR CP-2 Doppler radar. *Preprints, 24th Conference on Radar Meteorology*, Amer. Meteor. Soc., 236-239.
- Seliga, T.A., and V.N. Bringi, 1976: Potential use of radar reflectivity at orthogonal polarizations for measuring precipitation. *J. Appl. Meteor.*, **15**, 69-76.
- Spilhaus, A.F., 1948: Raindrop size, shape, and falling speed. *J. Meteor.*, **5**, 108-110.

- Stout, G.E., and S.A. Changnon, Jr., 1968: Climatography of hail in the central United States. Crop Hail Insurance Actuarial Association, Research Report 38.
- Ulbrich, C.W., and D. Atlas, 1982: Hail parameter relations: a comprehensive digest. *J. Appl. Meteor.*, **21**, 22-43.
- Wilson, J.W., 1975: Radar-gage precipitation measurements during the IFYGL. The Center for the Environment and Man Inc., Report 4177-540.
- Woodley, W., and A. Herndon, 1970: A rain gage evaluation of the Miami reflectivity-rainfall relation. *J. Appl. Meteor.*, **9**, 258-263.
- \_\_\_\_\_, A. Olsen, A. Herndon, and V. Wiggert, 1975: Comparison of gage and radar methods of convective rain measurement. *J. Appl. Meteor.*, **14**, 909-928.

which adequately covered storms in the Denver area from the CHILL location on June 6, i.e. the radar beam passes above lower levels.

### C. Summary

The application of Z-R relationships lead to overestimates by the radar during this storm, with radar rain totals too high at 31 of the 41 gages. The large radar rainfall overestimates during this event, as high as 58.8 mm (2.31 in) at gage 540, make this information of questionable usefulness in making urban flood forecasts in this case.

The NEXRAD default Z-R relation ( $Z = 300R^{1.4}$ ) resulted in even larger errors than the Colorado relation ( $Z = 500R^{1.3}$ ). A relation based on the Marshall-Palmer dropsize distribution ( $Z = 200R^{1.6}$ ) produced the best results, illustrating the difficulty in selecting the proper Z-R relation in advance.

The largest overestimates appeared to be associated with regions of hail. Hail was suggested by high ( $> 50$  dBZ) reflectivity values, near-zero  $Z_{DR}$  values, positive hail detection signal ( $H_{DR}$ ), and large deviations from the rain line at low levels. Using a reflectivity threshold to account for the effects of hail resulted in better radar rainfall estimates during this storm. A 50 dBZ threshold improved the average storm total G/RA from 0.77 to 0.92. Applying this technique to a storm with high reflectivity values and no hail would result in large errors, however.

## CHAPTER V

### RESULTS FOR THE AUGUST 5, 1991 DENVER THUNDERSTORM

#### A. Storm Characteristics

Conditions on August 5, 1991 once again were favorable for storm development in the Denver area. Ample amounts of low- and mid-level moisture were available, with dewpoint depressions less than 5°C from 524 mb to 433 mb and a surface dewpoint of 10.8°C at the 12 Z sounding. The afternoon temperature sounding indicated weakly unstable conditions, with a lifted index of +4 and a K index of 30.5.

Thunderstorms developed in the Denver vicinity by early afternoon and moved toward the east at 20 km/h. One hour of radar data, beginning at 1645 MDT, was examined for this event. The thunderstorm was located just to the west of central Denver at 1645 MDT and displayed peak reflectivity values of 48 dBZ. As the storm proceeded to the east, it developed into a northwest-to-southeast oriented line approximately 25 km long, with Z values up to 52 dBZ.

#### B. Rainfall Measurements

##### 1. Storm evolution

Figures 5.1–5.4 show the evolution of the rainfall pattern as derived from gage measurements and radar estimates. All radar estimates are made with the CO relation and no threshold unless indicated otherwise. During the first period

(1645-1700 MDT) the heaviest rain fell in western Denver near Interstate 25 (Figure 5.1a). Gages 600 and 1700 recorded 7.1 mm and 4.1 mm, respectively. The radar showed the heaviest rain to be in the same area, but underestimated, with estimates of 2.4 mm and 2.1 mm at gages 600 and 1700, respectively (Figure 5.1b). It should be noted that during periods 1 and 2 the storm primarily effected the sparsely instrumented western portion of the grid. Much of the detail of the rain pattern was missed during the first 30 minutes, but the situation improved as the storm moved over the densely gaged eastern portion of the network.

Rainfall peaked during period 2 (1700-1715 MDT), with 24.6 mm (0.97 in) recorded at gage 1720 (Figure 5.2a). The radar indicated only 7.4 mm (0.29 in) at this location (Figure 5.2b), an underestimate of 17.2 mm (0.68 in) in only 15 minutes. The location of the heaviest rain shifted 5 km to the northeast of its location during period 1. The region of the most intense rain was accurately determined by the radar.

During the third period (1715-1730 MDT), the region of heaviest rain became elongated toward the southeast as the storm moved eastward (Figure 5.3a). This region stretched from gage 1720, where 12.2 mm (0.48 in) fell, to gage 520, where 13.2 mm (0.52 in) was recorded. Once again the radar estimates were generally too low, especially for gages receiving heavier rain amounts: 8 out of 9 gages receiving 2.0 mm of rain or more were underestimated. Figure 5.3b shows that the radar completely missed the area of heavy rain near gages 1720 (gage: 12.2 mm, radar: 0.6 mm) and 530 (gage: 14.2 mm, radar: 1.6 mm). The underestimates of 12.6 mm (0.50 in) at gage 530 and 11.6 mm (0.46 in) at gage 1720 were certainly significant for such a short time period.

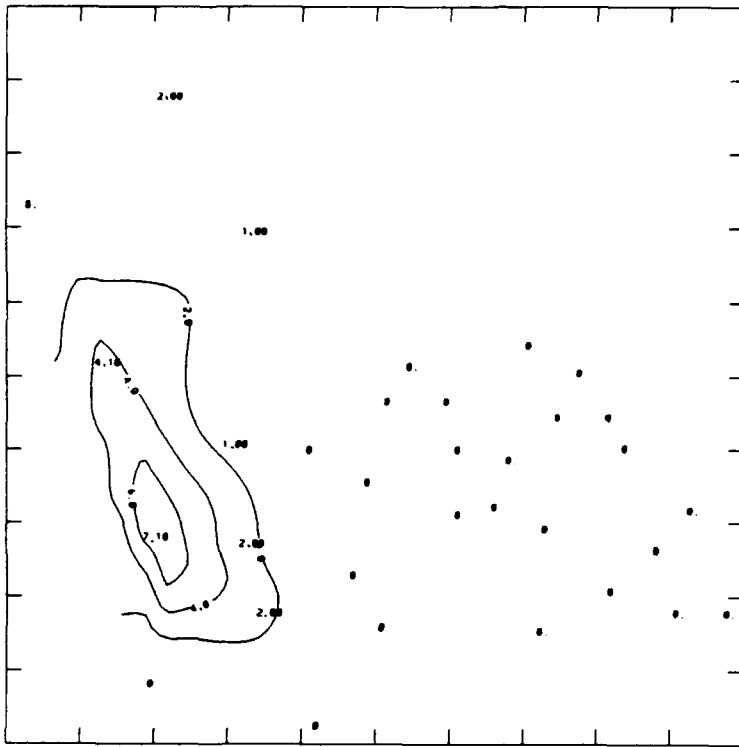


Figure 5.1a.

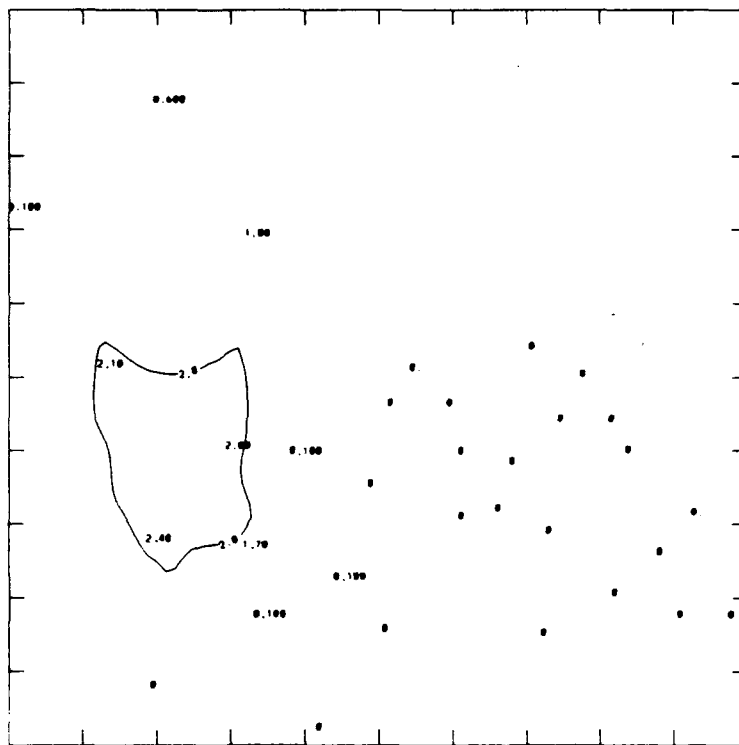


Figure 5.1b.

Figure 5.1. Rainfall (mm) for 1645-1700 MDT determined from a) rain gages and b) radar using  $Z = 500 R^{1.3}$  and no threshold.

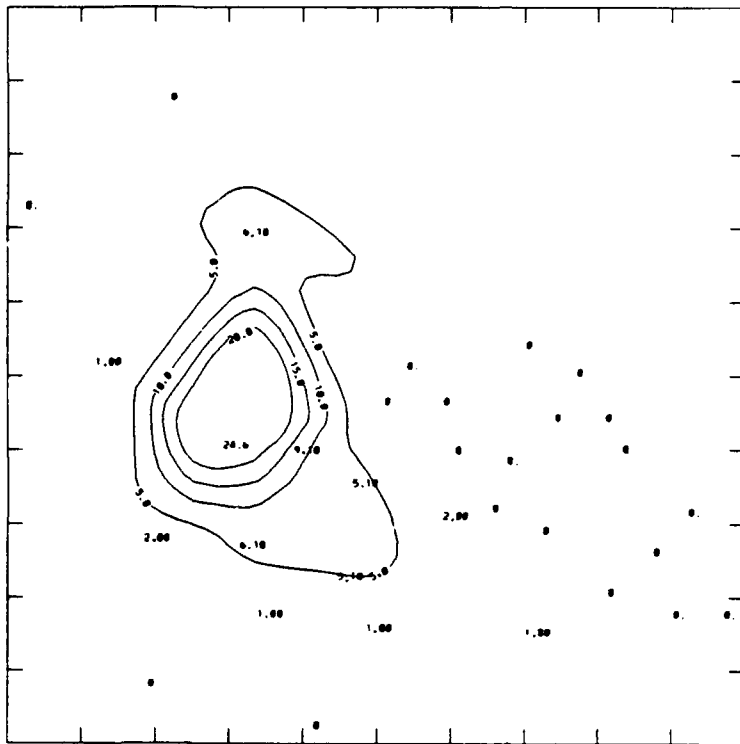


Figure 5.2a.

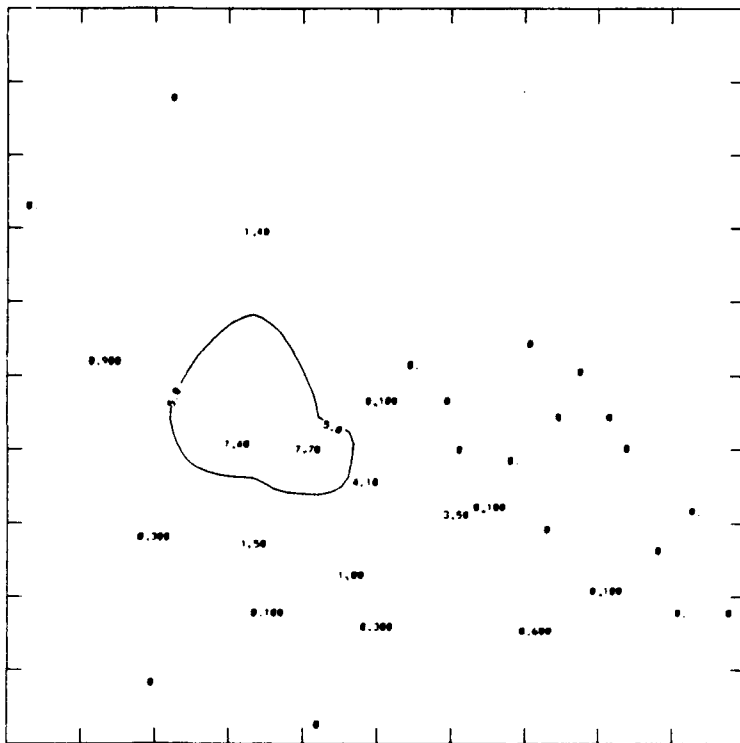


Figure 5.2b.

Figure 5.2. Same as Fig. 5.1, but for 1700-1715 MDT.



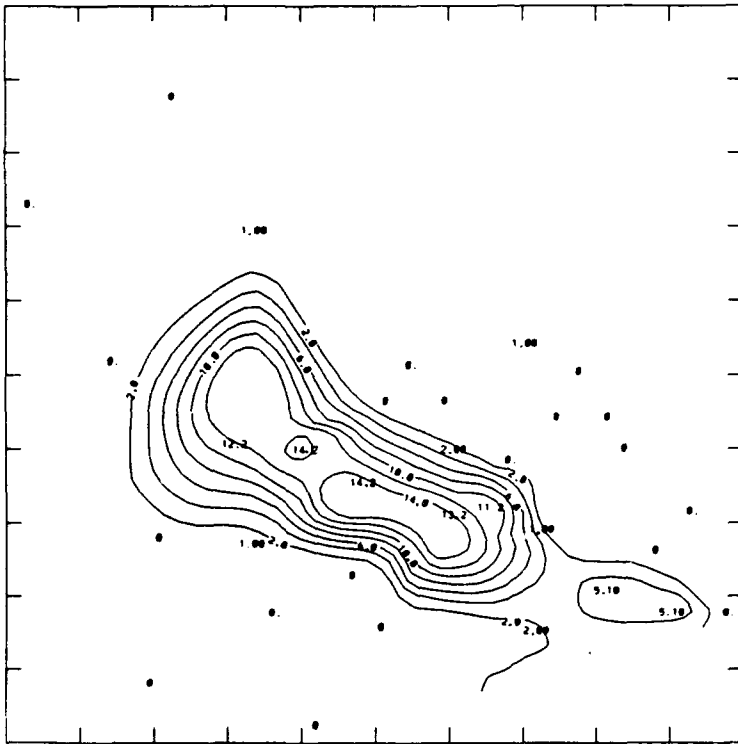


Figure 5.3a.

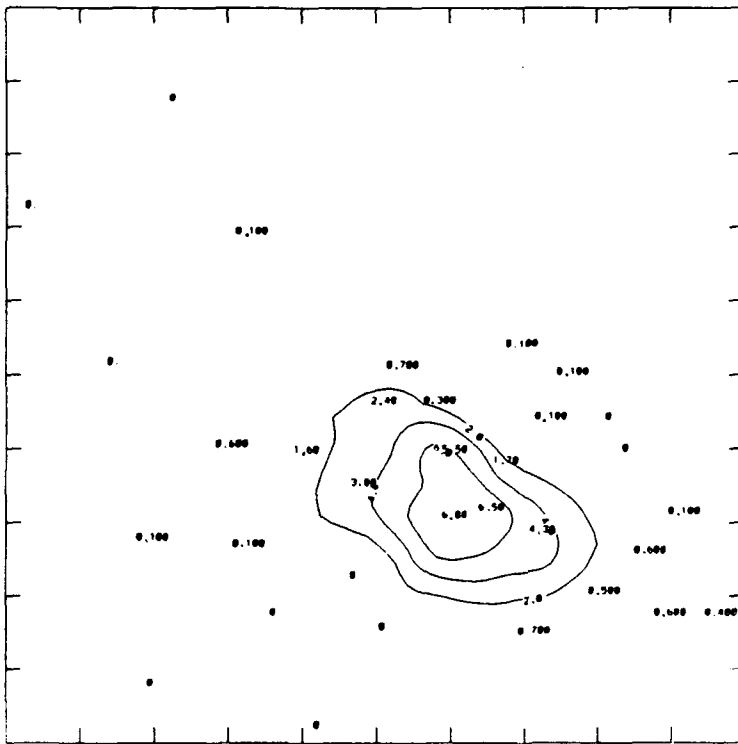


Figure 5.3b.

Figure 5.3. Same as Fig. 5.1, but for 1715-1730 MDT.

The general trend of radar rainfall underestimation continued as the storm dissipated during the final period (1730-1745 MDT). Gages 420 and 520 in Aurora recorded the peak rainfall value of 6.1 mm (0.24 in); see Figure 5.4a. An area of rainfall greater than 5.0 mm (0.20 in) extended to the southeast as far as gage 760. Figure 5.4b shows the extent of the radar underestimates. Of the 12 gages which received at least 2.0 mm of rain, 11 are underestimated. The peak underestimate of 5.8 mm (0.23 in) occurred at gage 520.

The heaviest total rainfall (1645-1745 MDT) fell south of Denver, with 37.8 mm (1.49 in) at gage 1720. Amounts over 15 mm (0.59 in) fell south of Lowry AFB and in southern Aurora (Figure 5.5a). No reports of street flooding, hail, or other severe weather were recorded. In sharp contrast to the June 6 storm, rainfall amounts were badly underestimated by the radar during this storm. Figure 5.5b shows radar rainfall estimates using  $Z = 500R^{1.3}$  and no threshold. The peak radar rainfall estimate was 10.8 mm at gage 520, an underestimate of 10.5 mm (0.43 in). Gage 1720, location of the peak gage rain, was underestimated by 27.8 mm (1.09 in) during the 1 hour study period. Rain amounts were underestimated for 22 out of 33 gages, with errors greater than 10 mm (0.39 in) at four gage locations. Radar underestimates are pervasive, except for a band of overestimates in the light rainfall region on the northern edge of the storm.

Figures 5.6a-b provide another picture of the temporal evolution of the rainfall pattern. During the first period, as many gage amounts were overestimated as underestimated by the radar (Figure 5.6a), but Figure 5.6b shows the underestimates were much larger. The number of gages underestimated increased during the second period as the storm intensified and began to move over the denser portion of the

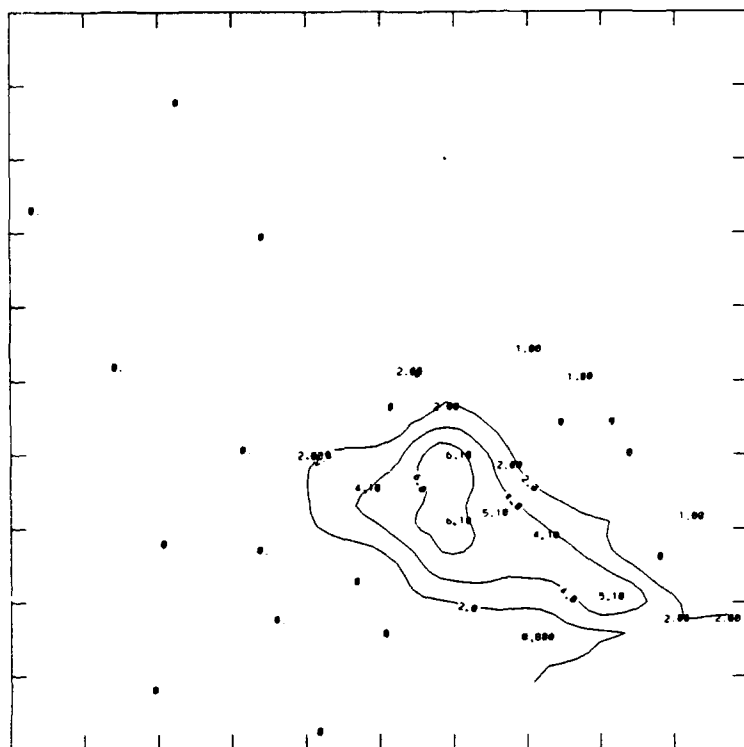


Figure 5.4a.

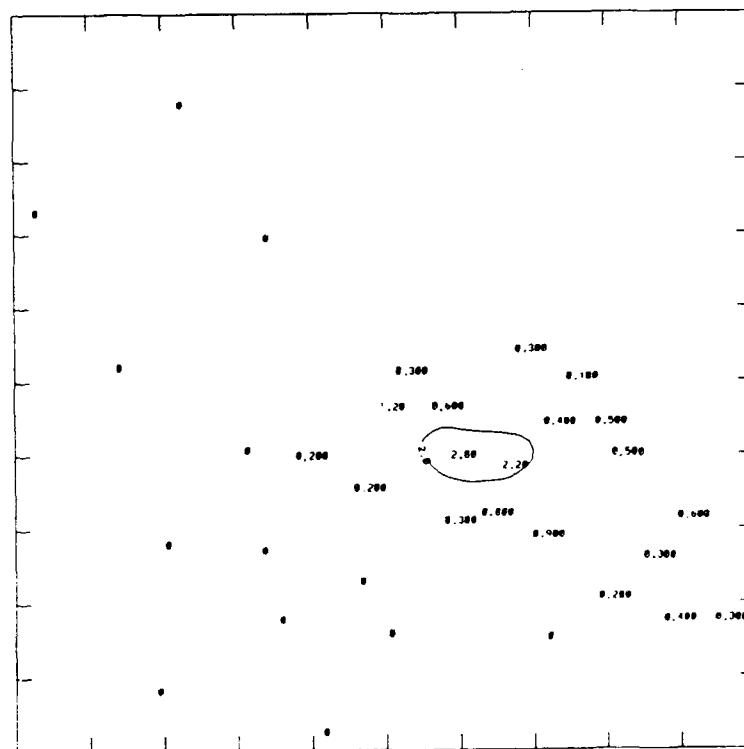


Figure 5.4b.

Figure 5.4. Same as Fig. 5.1, but for 1730-1745 MDT.



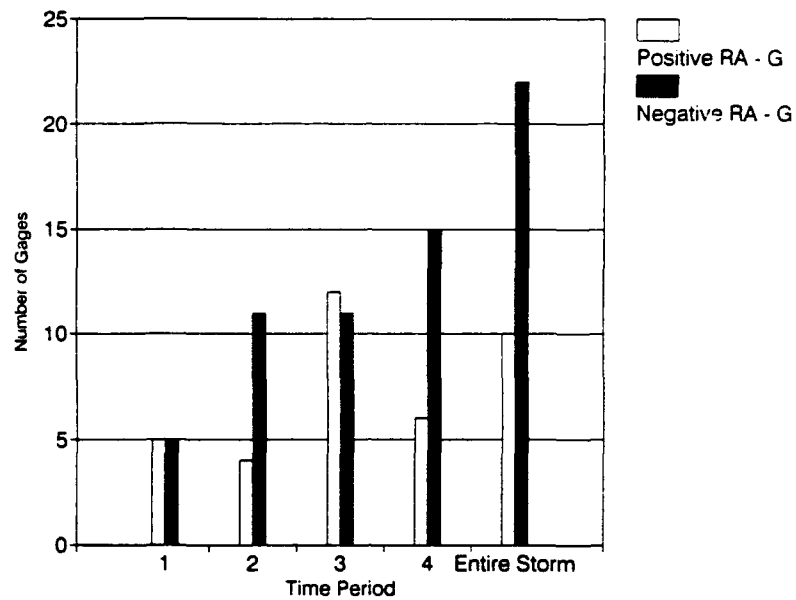


Figure 5.6a. Number of gages overestimated and underestimated by the radar during periods 1 (1645-1700), 2 (1700-1715), 3 (1715-1730), 4 (1730-1745), and the entire storm (1645-1745). All times in MDT.

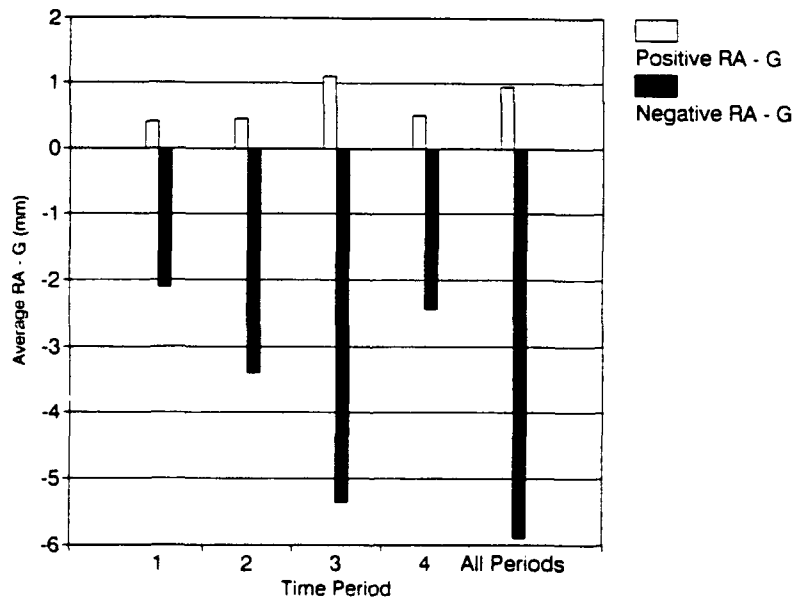


Figure 5.6b. Average difference (RA - G) in mm during the same periods as above.

gage network. The number of radar overestimates was actually larger than the number of underestimates by the third period. This was probably due to outflow winds on the northern edge of the storm, as discussed previously. The average magnitude of the radar underestimates remained larger than that of the overestimates, however. The decay of the storm during the fourth period was reflected in the smaller magnitude of the underestimates. For the storm as a whole, radar underestimates clearly were the rule.

## 2. Other Z-R relations

These results were improved slightly by using NR ( $Z = 300R^{1.4}$ ). The radar estimate at gage 520 increased to 12.1 mm (0.48 in), an underestimate of 9.2 mm (0.36 in). The error for gage 1720 was decreased somewhat, but was still large, with a deficiency of 26.5 mm (1.04 in). In general, NR improved radar estimates by 5-10%. In this case the CO relation, which was intended to help account for evaporation below the cloud base, actually lead to larger errors than NR, which was developed for the Miami area. MP ( $Z = 200R^{1.6}$ ) gave lower rainfall estimates in areas of moderate and heavy rain, but yielded higher estimates in regions of light rain.

Figure 5.7 shows the average G/RA for the three Z-R relations examined. MP gave the best overall results, while CO performed the worst. MP also performed the best for light ( $G < 5\text{mm}$ ) rain amounts, while NR gave the best results for the heavy ( $G > 11.9\text{ mm}$ ) rain category. It should be noted that these G/RA averages were biased somewhat by a few very large G/RA values at gages 620 and 760. The CO relation yielded overall G/RA values of 25.5 and 14.0 at gages 620 and 760,

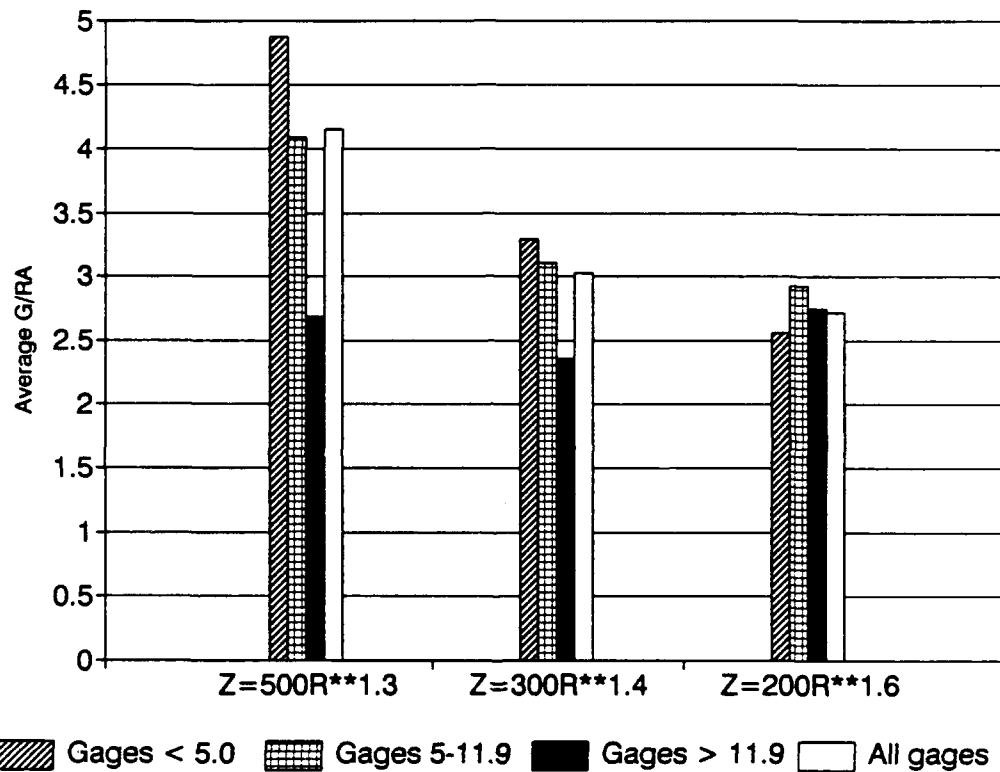


Figure 5.7. Average values of G/RA for the entire study period (1645-1745 MDT) using three Z-R relations. Gage amounts are divided into four categories: < 5.0 mm, 5-24.9 mm, 25.0 mm and above, and all gage amounts.

respectively. Ignoring these gages gave an overall average G/RA of 2.79, compared to 4.15 if these gages are included. These unusually high G/RA values also effected the results for the light and moderate rainfall categories. This effect was also apparent for the NR (overall average G/RA reduced from 3.03 to 2.16) and MP (G/RA reduced from 2.72 to 2.11). Even when gages 620 and 760 are ignored, the large radar underestimates (high G/RA) during this storm are a marked contrast to the overestimates (low G/RA) during the June 6 event (see Figure 4.11).

### C. Hail Indicators

#### 1. Reflectivity thresholds

Although this storm did produce reflectivity values up to 52 dBZ, only 20 pixels out of 14,000 had reflectivity values above 50 dBZ. Regions with reflectivity values above 50 dBZ were generally small (7 km<sup>2</sup> maximum) and had weakened greatly by the next scan. Radar estimates at each gage were not changed by applying a 50 dBZ threshold, although nearby pixels were reduced 1-2 mm in some cases. For example, the pixel just to the northwest of gage 1720 was reduced from 15.0 to 13.0 mm, a change of 13.3%. Rainfall estimates were reduced by 10-20% at ten other pixels. Although none of the radar estimates for particular gages were changed, it is apparent that a threshold would only increase the radar rainfall estimate errors for this storm.

#### 2. Differential Reflectivity ( $Z_{DR}$ ) and Hail Detection Signal ( $H_{DR}$ )

As noted in the previous chapter, once reflectivity values exceed 50 dBZ, hail typically occurs in Colorado thunderstorms (Kelsch, 1988 and 1989). Although small regions briefly met this criteria during the August 5 storm, the differential reflectivity



fields at these times did not suggest the presence of hail. The average  $Z_{DR}$  for the 20 pixels with  $Z > 50$  dBZ was 2.4 dB, with a range of 1.7 to 2.9 dB. These values are not indicative of hail.

The generally lower  $Z$  values and higher values of  $Z_{DR}$ , as compared to June 6, suggest in advance that the hail detection signal ( $H_{DR}$ ) will not indicate hail. Using the method discussed in Chapter 4,  $H_{DR}$  fields were generated for each of the 14 scans to confirm this. On August 5 the freezing level was approximately 4.6 km MSL, while complete radar coverage was obtained using a CAPPI at 3.0 km MSL. Because of this, the possibility of contamination by other frozen hydrometeors is much less than for the June 6 event, when the freezing level was 3.8 km MSL and a 3.5 km MSL CAPPI was used. A total of 8 pixels showed positive  $H_{DR}$  values on August 5, with the highest being 6.0 dB during scan 10 (1657:49–1702:36 MDT). The  $Z$  and  $Z_{DR}$  values at this point were 41 dBZ and 0.4 dB, respectively. Five other positive  $Z_{DP}$  values (2 pixels = 2.0 dB and 2 pixels = 1.0 dB) appeared during this scan, all with  $Z$  less than 40 dBZ. The three remaining positive  $Z_{DP}$  values were 2.0 dB or less, with one pixel in scans 8, 9, and 15. Although  $H_{DR}$  values during scan 10 may indicate a small region affected by hail, its presence was minimal and did not appear to have an effect on rainfall rates.

### 3. Difference Reflectivity ( $Z_{DP}$ )

The hail indicators discussed so far show very little evidence of the presence of hail, therefore a plot of  $Z_{DP}$  versus  $Z$  at 2.5 km MSL (well below the 4.6 km MSL 0°C level) is expected to be linear in nature. Figure 5.8a shows this to be the case for scan 8 (1648:08–1652:56 MDT), with 75 reflectivity values ranging from 21 to 48

dBZ plotted. This rain line is used, as in Chapter 4, to find the rain fraction and the deviation from the rain line at various levels. Figure 5.8b shows the change in the rain fraction ( $f$ ) with height during scan 8. Note the much less dramatic decline in the rain fraction with height compared to the June 6 storm (see Figure 4.23c). The deviation from the rain line (Figure 5.8c) also increases much more slowly, reaching 6.8 dB at 6.4 km AGL, compared to a value of 15.6 dB at the same level during the June 6 event (see Figure 4.23b).

#### D. Summary

In contrast to the June 6 storm, radar rainfall was underestimated during this event. Radar rainfall estimates were too low at 22 of the 33 gages, with a peak underestimate of 27.8 mm (1.09 in) at gage 1720.

The NR Z-R relation provided some improvement over the CO relation, giving estimates generally 5-10% closer to the gage amounts. The CO relation produced the largest errors of all the relations studied, while the MP relation performed the best.

Hail was not indicated by  $Z_{DR}$  and  $H_{DR}$  fields, nor by the deviation from the rain line at low levels. Small, short-lived regions of reflectivity above 50 dBZ did exist, however. Applying a reflectivity threshold to this storm would only result in larger errors than those already evident.

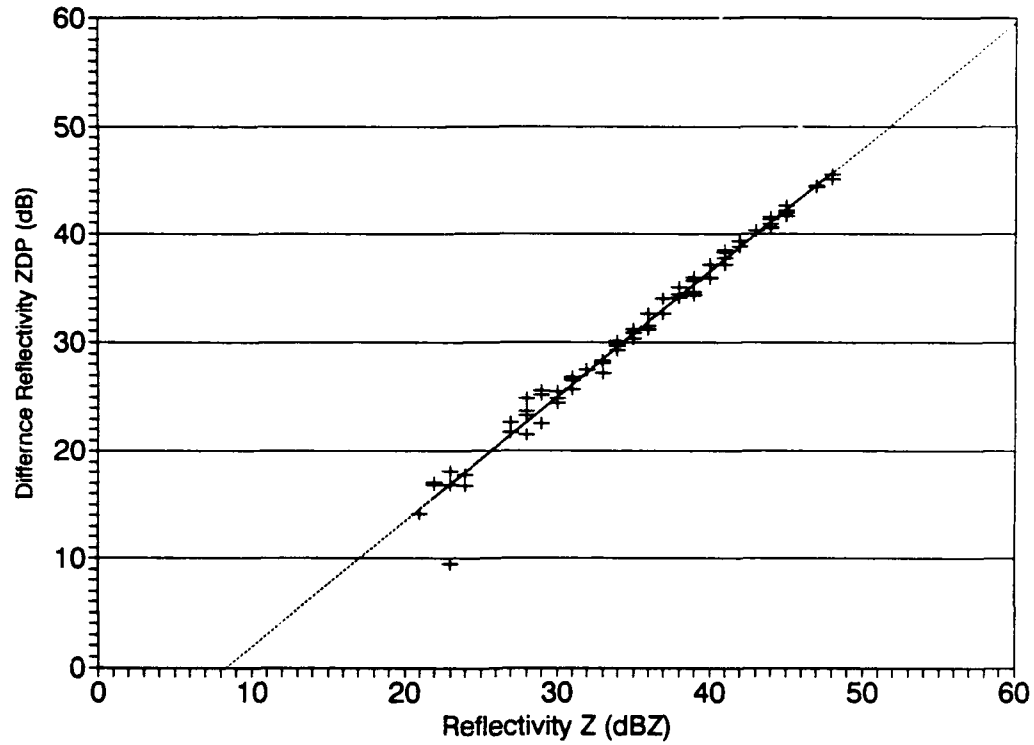


Figure 5.8a. Scatter plot of  $Z_{DP}$  versus  $Z_H$  for scan 8 at 2.5 km MSL. This plot is composed of 75  $Z_H$ ,  $Z_{DP}$  pairs.

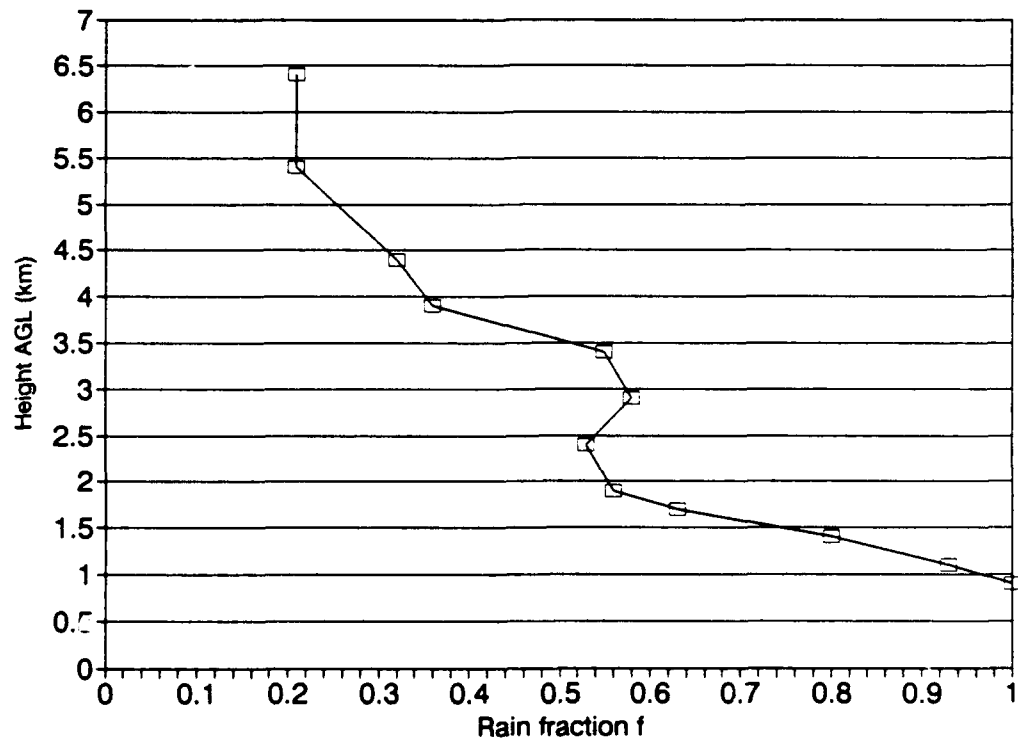


Figure 5.8b. Rain fraction,  $f$  as a function of height (km AGL) during scan 8. The  $0^{\circ}\text{C}$  level is 3.0 km AGL.

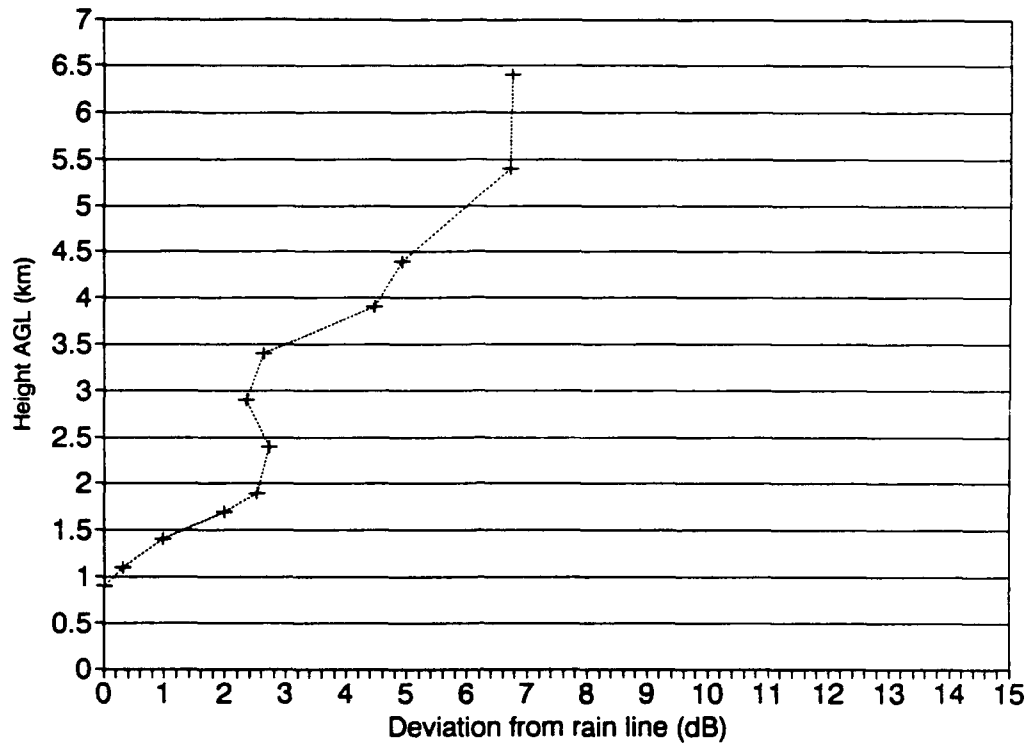


Figure 5.8c. Deviation from the rain line as a function of height (km AGL) during scan 8. The 0°C level is 3.0 km AGL.

## CHAPTER VI

### CONCLUSIONS

It has long been hoped that rainfall measurements made with weather radars would be able to supplement or even replace rain gage networks. Provided the rainfall estimates of the radar are of sufficient accuracy, the 1296 data points the radar provides over this particular study area would be a tremendous improvement over the 41 rain gages in the present network. Unfortunately, estimates of rainfall by radar were frequently in error by large amounts. The radar estimate for gage 540 during the June 6 storm was 58.8 mm (2.31 in) higher than the gage amount, an error of 201%. During the August 5 event gage 1720 recorded 37.8 mm, while the radar estimate was 27.8 mm (1.09 in) lower. Such large errors are not acceptable for most meteorological or hydrological purposes. The use of different Z-R relations provided overall improvement during both storms, while reflectivity thresholds resulted in better estimates during the June 6 storm, where hail was present. While better radar rainfall estimates can be realized by varying the Z-R relation and/or by accounting for hail with a reflectivity cap, these methods are difficult to apply in real time. This is especially true for radars without a dual-polarization capability to help detect hail, a feature the new NEXRAD network will lack.

During the June 6 storm, the largest overestimates were associated with unusually high reflectivity values resulting from the presence of hail. Hail was inferred from an examination of  $Z$ ,  $Z_{DR}$ ,  $H_{DR}$ , and  $Z_{DP}$  fields. Values of  $Z > 50$

dBZ, near-zero  $Z_{DR}$  measurements, positive  $H_{DR}$  values, and  $Z_{DP}$  values deviating from the rain line all provided evidence for the presence of hail. Using a reflectivity threshold of 50 dBZ, in an attempt to account for hail contamination, improved the average G/RA from 0.77 to 0.92. The average difference improved from 8.0 mm to 3.5 mm, while the average percentage difference dropped from 87.5% to 54.4%.

Even though overall results improved with the use of a threshold during the June 6 event, the danger of badly underestimating rainfall in a storm with values above 50 dBZ and no hail is very real. This is shown to be the case during the August 5 event: rainfall estimates were too low without a threshold, a 50 dBZ cap only increased the errors. The more sophisticated hail detection techniques based on polarimetric radar measurements ( $Z_{DR}$ ,  $H_{DR}$ , and  $Z_{DP}$ ) could be used to determine whether a simple reflectivity threshold should be applied or not. A storm producing rain alone will be discernible using the methods mentioned above. This is indeed the case during the August 5 storm, where  $Z_{DR}$ ,  $H_{DR}$ , and  $Z_{DP}$  measurements all indicated the absence of hail. Therefore, these measurements indicated in advance that using a reflectivity cap would be unwise. Even radars able to make polarimetric measurements cannot account for the effects of evaporation and wind drift below the beam level, however this study confirms what many previous studies have shown: radar rainfall estimates using the Z-R relations tested here provide good supplemental information, but will not completely replace traditional rain gages.

## CHAPTER VII

## REFERENCES

- Ahnert, P., M. Hudlow, E. Johnson, D. Green, and M. Dias, 1983: Proposed "on-site" precipitation processing system for NEXRAD. *Preprints, 21st Radar Meteorology Conference*, Amer. Meteor. Soc., 378-385.
- Albers, S., K. Heideman, R. Jesuroga, M. Kelsch, J. Smart, J. Snook, E. Szoke, D. Walker, and H. Winston, 1988: PROFS final report to NEXRAD/JSPO for the 1988 fiscal year. NOAA/ERL/FSL/PROFS, Boulder, CO, 27-44.
- Atlas, D., and A.C. Chmela, 1957: Physical-synoptic variations of raindrop size parameters. *Preprints, Sixth Weather Radar Conference*, Cambridge, MA. Amer. Meteor. Soc., 21-29.
- Atlas, D., and C.W. Ulbrich, 1990: Early foundations of the measurement of rainfall by radar. Chapter 12 in *Radar in Meteorology*, D. Atlas, Ed.), Amer. Meteor. Soc., Boston, MA.
- Aydin, K., and T.A. Seliga, 1984: Radar polarimetric backscattering properties of conical graupel. *J. Atmos. Sci.*, **41**, 1887-1892.
- \_\_\_\_\_, K., \_\_\_\_\_, and V. Balaji, 1986: Remote sensing of hail with dual linear polarization radar. *J. Climate Appl. Meteor.*, **25**, 1475-1484.
- \_\_\_\_\_, K., Y. Zhao, and T.A. Seliga, 1990: A differential reflectivity radar hail measurement technique: Observations during the Denver hailstorm of 13 June 1984. *J. Atmos. Oceanic Tech.*, **7**, 104-113.
- Balakrishnan, N. and D.S. Zrnic, 1990a: Estimation of rain and hail rates in mixed-phase precipitation. *J. Atmos. Sci.*, **47**, 565-583.
- \_\_\_\_\_ and \_\_\_\_\_, 1990b: Use of polarization to characterize precipitation and discriminate large hail. *J. Atmos. Sci.*, **47**, 1525-1540.
- Battan, L.J., 1973: *Radar Observation and the Atmosphere*. University of Chicago Press, Chicago IL.

- Brandes, E.A., and J.W. Wilson, 1986: Measuring storm rainfall by radar and rain gage. In **Thunderstorms: A Social, Scientific, and Technological Documentary**. Vol. 3: Instruments and Techniques for Thunderstorm Observation and Analysis (E. Kessler, Ed.), Second ed., University of Oklahoma Press, Norman, OK.
- Bringi, V.N., R.M. Rasmussen and J. Vivekanandan, 1986: Multiparameter radar measurements of Colorado convective storms, Part I: Graupel melting studies. *J. Atmos. Sci.*, **43**, 2345-2563.
- Burgess, D., and P.S. Ray, 1986: Principles of Radar. In *Mesoscale Meteorology and Forecasting* (P.S. Ray, Ed.), American Meteorological Society, Boston, MA.
- Dahlstrom, B., 1973. Investigation of errors in rainfall observations: a continued study. Report 34, Department of Meteorology, University of Uppsala, Sweden.
- Doviak, R., and D. Zrnić, 1984: **Doppler Radar and Weather Observations**. Academic Press, Orlando, FL, 480 pp.
- Doviak, R., D. Sirmans, and D. Zrnić, 1986: Weather radar. In **Thunderstorms: A Social, Scientific, and Technological Documentary**. Vol. 3: Instruments and Techniques for Thunderstorm Observations and Analysis (E. Kessler, Ed.), Second ed., University of Oklahoma Press, Norman, OK.
- Golestani, Y., V. Chandrasekar and V.N. Bringi, 1989: Intercomparison of multiparameter radar measurements. *Proc. 24th AMS Conference on Radar Meteorology, Amer. Meteor. Soc.*, 309-314.
- Jameson, A.R., 1983: Microphysical interpretation of polarization measurements in rain, Part I: Interpretation of polarization measurements and estimation of raindrop shapes. *J. Atmos. Sci.*, **40**, 1792-1802.
- Jones, D.M.A., 1966: The correlation of raingage-network and radar-detected rainfall. *Preprints, Twelfth Conference on Radar Meteorology*, Norman, OK. Amer. Meteor. Soc., 204-207.
- Joss, J., and A. Waldvogel, 1990: Precipitation measurement and hydrology. Chapter 29a in *Radar in Meteorology* (D. Atlas, Ed.), Amer. Meteor. Soc., Boston, MA.
- Kelsch, M., 1988: A meteorological assessment of the NEXRAD hydrology sequence for thunderstorms producing heavy rain. *Preprints, 15th Conference on Severe Local Storms, Amer. Meteor. Soc.*, 209-212.



- \_\_\_\_\_, 1989: An evaluation of the NEXRAD hydrology sequence for different types of convective storms in northeastern Colorado. *Preprints, 24th Conference on Radar Meteorology*, Amer. Meteor. Soc., 207-210.
- Knight, N.C., 1986: Hailstone shape factor and its relation to radar interpretation of hail. *J. Climate Appl. Meteor.*, **25**, 1956-1958
- Larson, L.W., and E.L. Peck, 1974: Accuracy of precipitation measurements and hydrologic modeling. *Water Resour. Res.*, **10**, 857-863.
- Lipschutz, R.C., J.F. Pratte, and J.R. Smart, 1989: An operational  $Z_{DR}$ -based precipitation type/intensity product. *Preprints, 24th Conference on Radar Meteorology*, Amer. Meteor. Soc., 91-94.
- Mason, B.J., 1971: **The Physics of Clouds**. Clarendon Press, 672 pp.
- Marshall, J.S., and W.M. Palmer, 1948: The distribution of raindrops with size. *J. Meteor.*, **5**, 165-166.
- McCormick G.C., and B.L. Barge, 1972: The anisotropy of precipitation media. *Nature*, **238**, 214-216.
- Meischner, P.F., V. Bringi, D. Heimann, and H. Holler, 1991: A squall line in southern Germany: Kinematics and precipitation formation as deduced by advanced polarimetric and Doppler radar measurements. *Mon. Wea. Rev.*, **119**, 678-701.
- Mohr, C.G., L.J. Miller, and R.L. Vaughan, 1981: An interactive software package for the rectification of radar data to three-dimensional Cartesian coordinates. *Preprints, 21st Conference on Radar Meteorology*, Amer. Meteor. Soc., 569-574.
- NEXRAD, 1982: NEXRAD technical requirements (NTR). NEXRAD Joint System Program Office, Silver Spring, MD.
- NOAA, 1991: Preliminary Storm Data report, June 1991. WSFO Denver, CO.
- Rasmussen, E.N., J. Smith, J. Pratte, and R. Lipschutz, 1989: Real time precipitation accumulation estimation using the NCAR CP-2 Doppler radar. *Preprints, 24th Conference on Radar Meteorology*, Amer. Meteor. Soc., 236-239.
- Seliga, T.A., and V.N. Bringi, 1976: Potential use of radar reflectivity at orthogonal polarizations for measuring precipitation. *J. Appl. Meteor.*, **15**, 69-76.
- Spilhaus, A.F., 1948: Raindrop size, shape, and falling speed. *J. Meteor.*, **5**, 108-110.

- Stout, G.E., and S.A. Changnon, Jr., 1968: Climatology of hail in the central United States. Crop Hail Insurance Actuarial Association, Research Report 38.
- Ulbrich, C.W., and D. Atlas, 1982: Hail parameter relations: a comprehensive digest. *J. Appl. Meteor.*, **21**, 22-43.
- Wilson, J.W., 1975: Radar-gage precipitation measurements during the IFYGL. The Center for the Environment and Man Inc., Report 4177-540.
- Woodley, W., and A. Herndon, 1970: A rain gage evaluation of the Miami reflectivity-rainfall relation. *J. Appl. Meteor.*, **9**, 258-263.
- \_\_\_\_\_, A. Olsen, A. Herndon, and V. Wiggert, 1975: Comparison of gage and radar methods of convective rain measurement. *J. Appl. Meteor.*, **14**, 909-928.